1968-5

A Similarity Model for Flow in a Turbulent Boundary Layer

Earl Clark Lemmon
Brigham Young University - Provo

A SIMILARITY MODEL FOR FLOW IN A TURBULENT BOUNDARY LAYER

A Thesis

Presented to the

Department of Mechanical Engineering Science

Brigham Young University

In Partial Fulfillment

of the Requirements for the Degree

Master of Science

by

E. Clark Lemmon

May 1968

This thesis, by E. Clark Lemmon, is accepted in its present form by the Department of Mechanical Engineering Science of Brigham Young University as satisfying the thesis requirement for the degree of Master of Science.

2 MAY 1968

Date

Typed by: Nancy Lyn Tippetts

ACKNOWLEDGMENTS

The author wishes to express his appreciation to Dr. Charles Y. Warner and Dr. John N. Cannon for their technical suggestions and encouragement relating to this project and for their counsel in the preparation of this thesis.

TABLE OF CONTENTS

LIST OF FIGURES

NOMENCLATURE

A	arbitrary constant
C	constant of integration
f	$f(\eta)$
n	arbitrary constant
u	velocity in x direction
v	velocity in y direction
x	direction parallel to the plate
y	direction perpendicular to the plate
C_f	coefficient of friction
$f(\eta)$	function of η
f'	$\partial f(\eta)/\partial\eta$
Re_x	Reynolds number based on x
U_∞	free stream velocity
$\overline{u}$	time averaged mean velocity in x direction
u'	fluctuating velocity in x direction
u^*	shear velocity
u^+	dimensionless velocity
$\overline{v}$	time averaged mean velocity in the y direction
v'	fluctuating velocity in the y direction
$\overline{u'v'}$	time average of product of fluctuating velocities
y^+	dimensionless distance
δ	boundary layer thickness
$\Delta\eta$	step size
η	$y\sqrt{U_\infty/x\nu}$
μ_t	eddy viscosity

ν	kinematic viscosity or molecular diffusivity
ν_t	eddy diffusivity
ξ	x
ρ	density
τ	shear stress
τ_o	shear stress at wall
τ_t	Reynolds stress
Ψ_p	stream function for potential flow
Ψ_t	stream function for turbulent flow

CHAPTER I

INTRODUCTION

One of the basic goals in engineering is to generate models which will provide a means for analytically predicting observed phenomenon. Such a model is often modified several times to obtain better results. The purpose of this study was to generate a model for an equilibrium turbulent boundary layer for steady flow over a flat plate and compare the results obtained by using the model with experimental data. Part of the objective was to also suggest ways in which the model could be modified to obtain better results.

The significance of this project is that it provides a method to obtain a model of the variation of the eddy diffusivity across the boundary layer that will yield a velocity profile which is in agreement with experimental data.

The model of the eddy diffusivity across the boundary layer obtained will only be an approximation. However, since the simplified model of the eddy diffusivity will yield a good approximation to the velocity profile it will be useful. This model of the variation can then be used in other applications, such as the determination of the temperature profile in natural convection.

The model was generated by reducing the equation of motion from a partial differential equation to an ordinary differential equation by an affine transformation. A similarity solution similar to the solution obtained by Blasius for a laminar layer flowing over a flat plate was obtained. The transformed governing equation obtained was found to be dependent on the behavior of the eddy diffusivity within the boundary layer. The modeling of this behavior is of particular significance, and will be discussed later in detail. The results obtained with the model generated are compared with experimental data, and methods of improving the model are suggested.

CHAPTER II

BACKGROUND MATERIAL

Flow in a turbulent boundary layer is of major interest because it occurs in a large number of practical fluid and heat transfer problems.

The motion of the fluid is extremely complex; however there is a certain degree of regularity when the motion is viewed statically, without an attempt to describe the detailed motion of an individual particle. In the past, this statistical approach has been used by correlating a vast amount of experimental data. This without making an attempt to predict turbulent velocity profiles by application of the equations of motion.

For purely laminar flow the shear stress at any point in the boundary layer is given by

$$\tau = \rho\nu \frac{du}{dy}$$

In the region very near the wall the shear stress will vary only slightly from the shear stress at the wall, and thus in this region

$$\tau \approx \tau_0$$

Integrating and expressing the result in dimensionless form,

$$du = (\tau_0/\rho\nu)\, dy$$

$$u = (\tau_0/\rho\nu)\, y + C$$

$$u/\sqrt{\tau_0/\rho} = y\sqrt{\tau_0/\rho}/\nu + C$$

But at $y = 0$, $u = 0$, therefore $C = 0$ and the result is

$$u / \sqrt{\tau_0/\rho} = y \sqrt{\tau_0/\rho} / \nu$$

The term $\sqrt{\tau_0/\rho}$ is usually called the shear velocity since it has the dimensions of velocity and is denoted by u^*. The two dimensionless groups are usually represented by the symbols u^+ and y^+ where

$$u^+ = u / u^* \qquad \text{and} \qquad y^+ = y u^* / \nu$$

which gives for the region very near the wall in laminar flow

$$u^+ = y^+ \tag{1}$$

In a fully developed equilibrium turbulent boundary layer the flow is often divided into three different regions. The region in contact with the wall is termed the viscous sublayer. The intermediate region is often called the buffer zone and the outer region is usually referred to as the fully turbulent region.

Two laws that have given some order and meaning to turbulent flow data are the "law of the wall" attributed to Prandtl [1] and the "velocity defect law" introduced by von Karman [2]. The first pertains to the region close to the wall where the effect of viscosity is directly felt and the second pertains to the bulk of the shear layer or turbulent core where the viscous forces become negligible.

In the viscous sublayer the "law of the wall" postulates that the time-averaged velocity at a point in this region is a function primarily of local or near-local conditions and does not depend very strongly on conditions at some faraway point. A list of the measurable quantities upon which the time-averaged velocity in this boundary region might possibly depend should include the distance from the surface y; the shear stress at the surface, τ_0 ; and the viscosity and density of the fluid, ν and ρ . That is

$$\bar{u} = \bar{u}(y, \tau_0, \nu, \rho).$$

By application of dimensional analysis this relation can be reduced to a function of two dimensionless groups, as follows

$$\bar{u} / \sqrt{\tau_0/\rho} = f\left(y\sqrt{\tau_0/\rho}\,/\nu\right)$$

The two dimensionless groups are simply u^+ and y^+. This gives a final result

$$u^+ = f(y^+) \qquad (2)$$

which is known as the "law of the wall."

Assuming that all the pertinent variables have been included, the above relationship implies that if turbulent velocity profiles are measured over a wide range of Reynolds numbers it should be possible to plot u^+ versus y^+, and all the data should fall on a single curve.

The validity of Equation (2) for purely laminar flow has already been demonstrated. Here $f(y^+)$ is simply y^+.

Nikuradse [3] and others have observed that within the viscous sublayer that

$$u^+ = y^+$$

Hence, the viscous sublayer is laminar-like in that $u^+ = y^+$, as is true for a laminar boundary layer.

The "velocity defect law" postulates that the reduction in velocity $(U_\infty - u)$ at a distance y is the result of a tangential stress at the wall, independent of how this stress arises but dependent on the distance δ to which the effect has diffused from the wall. The form of the relationship is

$$U_\infty - \bar{u} = g\left(\sqrt{\tau_0/\rho},\, y,\, \delta\right)$$

which can be reduced by dimensional analysis to

$$(U_\infty - \bar{u})\Big/\sqrt{\tau_0/\rho} = g\,(y/\delta) \qquad (3)$$

This is the "velocity defect law."

Experimental results have shown that the regions of validity of the law of the wall and the velocity defect law overlap one another. Millikan [4] has shown that if there is any region of overlap in which both laws are valid, then the functions f and g must be logarithms. A simple way to arrive at this conclusion is to reexamine Equations (2) and (3), written in the following forms:

$$u/u^* = f\left[(y/\delta)(\delta u^*/\nu)\right]$$

$$u/u^* = U_\infty/u^* - g\,(y/\delta)$$

Since these are two expressions for the same quantity, and since a multiplying factor inside a function must have the same effect as an additive factor outside a function, the functions f and g must be logarithms. The first formula is usually written in the form

$$u^+ = k \log y^+ + C \qquad (4)$$

Kestin and Richardson [5] have plotted data from several different sources on u^+, y^+ coordinates. Their results appear in Figure 1. At very small values of y^+ the data tend to approach Equation (1), while for all y^+ greater than about twenty-five or thirty an equation of the form of Equation (4) fits the data very well.

Figure 2 shows three curves which have been proposed by various investigators to fit the experimental data shown in Figure 1. These investigators have described the universal turbulent velocity behavior

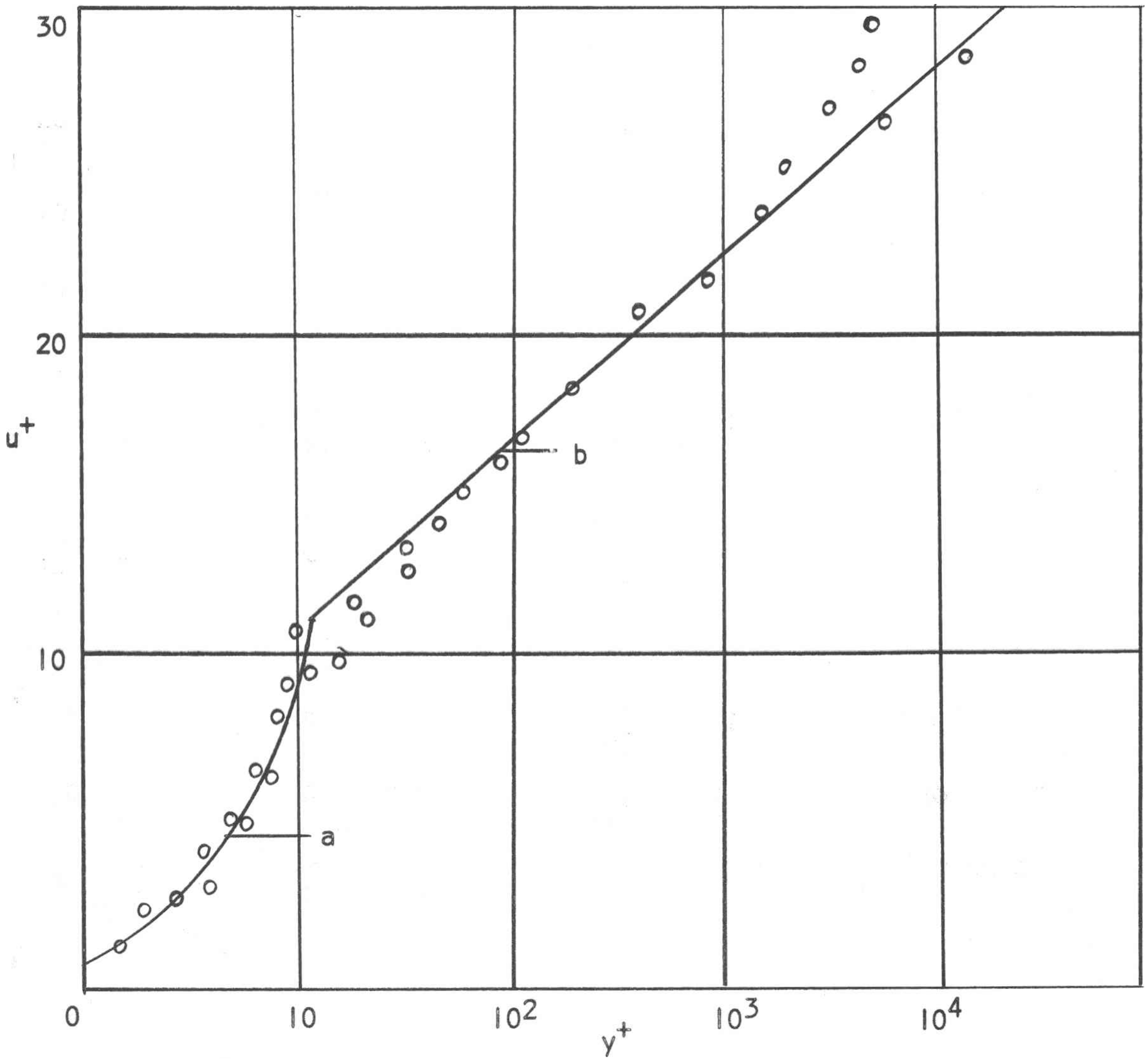

Fig. 1. -- Comparison of the law of the wall with experimental data. (After Kestin and Richardson [5])

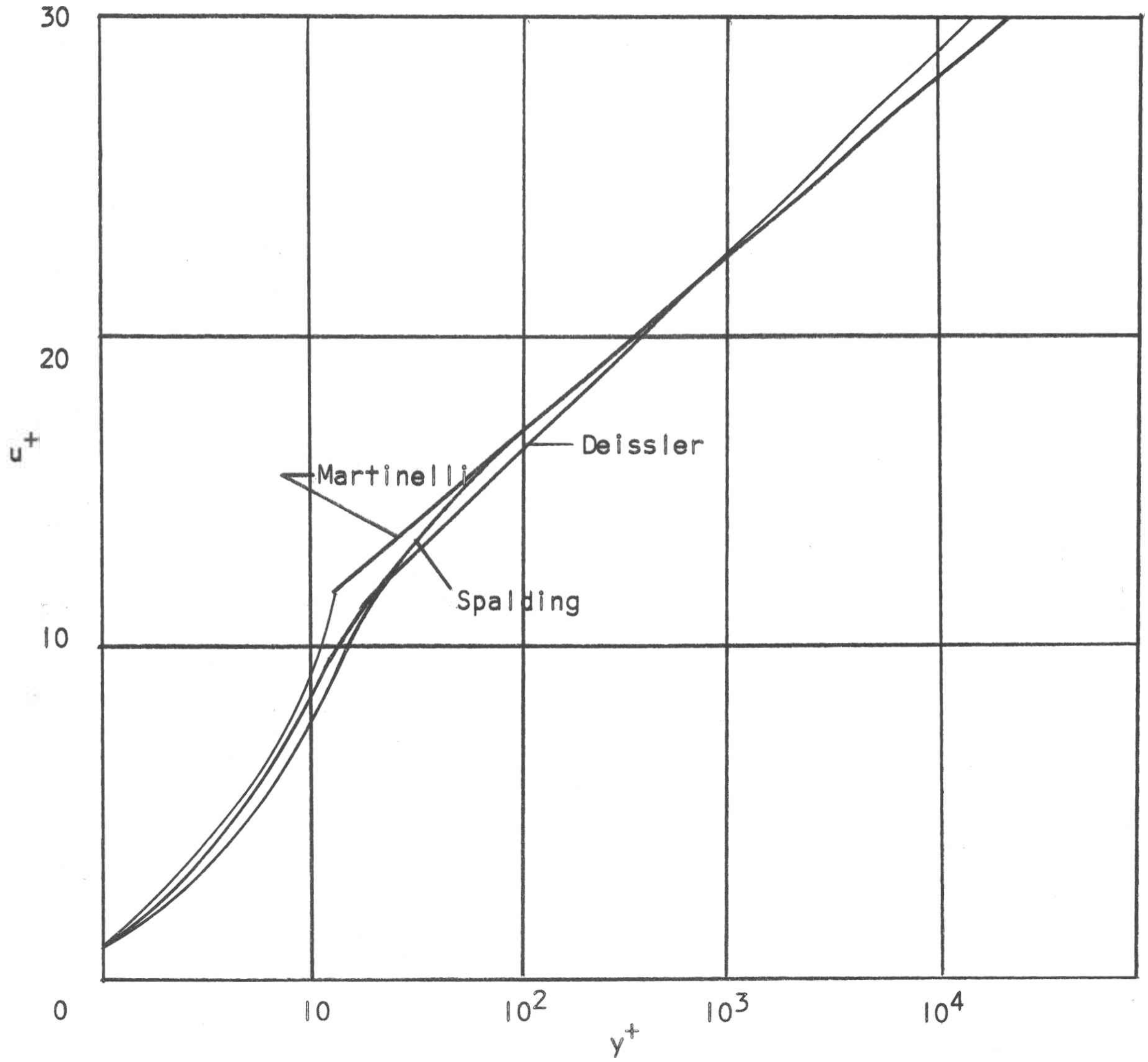

Fig. 2. -- Empirical representations of the law of the wall.

near the wall in terms of one, two, or three separate algebraic equations. Martinelli [6] gives three equations to represent the data. They are

$$\begin{aligned} &y^+ < 5 && u^+ = y^+ \\ &5 < y^+ < 30 && u^+ = -3.05 + 5.00 \ln(y^+) \\ &y^+ > 30 && u^+ = 5.5 + 2.5 \ln(y^+) \end{aligned} \tag{5}$$

Deissler [7], using Van Driest's [8] modification near the wall, gives two equations to fit the data which are

$$\begin{aligned} &y^+ < 26 && y^+ = \sqrt{\frac{\pi}{2(.0119)}}\, \exp\left(\frac{1}{2}(.0119)(u^+)^2\right) \operatorname{erf}\left(\sqrt{\frac{.0119}{2}}\, u^+\right) \\ &y^+ > 26 && u^+ = 3.8 + 2.78 \ln(y^+) \end{aligned} \tag{6}$$

Finally, Spalding [9] gives a single equation for all y^+, which is

$$y^+ = u^+ + \frac{1}{9.025}\left[e^{.4u^+} - 1 - (.4u^+) - \frac{(.4u^+)^2}{2!} - \frac{(.4u^+)^3}{3!} - \frac{(.4u^+)^4}{4!}\right] \tag{7}$$

CHAPTER III

MATHEMATICAL MODEL

If the density and viscosity are constant, and if the body forces and pressure gradient in the x direction are zero, the governing equations for steady two dimensional flow over a flat plate in a laminar boundary layer given by Schlichting [10] are

Continuity

$$\frac{\partial u}{\partial x} + \frac{\partial v}{\partial y} = 0 \qquad \text{and}$$

Momentum (x direction)

$$u\frac{\partial u}{\partial x} + v\frac{\partial u}{\partial y} = \nu \frac{\partial^2 u}{\partial y^2} \tag{8}$$

Subject to the boundary conditions

$$y = 0 \ : \ u = v = 0$$

$$y = \infty \ : \ u = U_\infty$$

These two equations can be combined to give

$$\frac{\partial u^2}{\partial x} + \frac{\partial uv}{\partial y} = \nu \frac{\partial^2 u}{\partial y^2} \tag{9}$$

Governing Equation

It is generally assumed that the motion in a turbulent boundary layer can be separated into a mean flow whose components are $\bar{u}$ and $\bar{v}$, and a superposed turbulent flow whose components are u' and v', the mean values of which are zero. Making this assumption the velocities become

$$u = \bar{u} + u'$$
$$v = \bar{v} + v'$$

Equation (9) then becomes

$$\frac{\partial}{\partial x}(\bar{u}+u')^2 + \frac{\partial}{\partial y}(\bar{u}+u')(\bar{v}+v') = \nu \frac{\partial^2}{\partial y^2}(\bar{u}+u') \qquad (10)$$

If Equation (10) is now time-averaged the resulting relationship is

$$\frac{\partial}{\partial x}(\bar{u})^2 + \frac{\partial}{\partial y}(\bar{u}\bar{v}) + \overline{\frac{\partial (u')^2}{\partial y}} + \overline{\frac{\partial}{\partial y}(u'v')} = \nu \frac{\partial^2 \bar{u}}{\partial y^2} \qquad (11)$$

Comparing Equation (11) with Equation (9) shows that two terms are added as a consequence of turbulence. Experimental results [11] have shown that

$$\frac{\partial \overline{(u')^2}}{\partial x} << \frac{\partial \overline{(u'v')}}{\partial y}$$

Equation (11) then becomes when rearranged

$$\frac{\partial}{\partial x}(\bar{u})^2 + \frac{\partial}{\partial y}(\bar{u}\bar{v}) = \nu \frac{\partial^2 (\bar{u})}{\partial y^2} - \frac{\partial \overline{(u'v')}}{\partial y} \qquad (12)$$

and is called the mean momentum equation with fluctuations. If the turbulent momentum flux (τ_t) or Reynolds stress is defined as

$$\tau_t = -\rho\, \overline{(u'v')}$$

Then by analogy to the laminar momentum flux

$$\tau_t = -\mu_t \frac{\partial \bar{u}}{\partial y}$$

where

$$\mu_t = -\rho \overline{u'v'} / [\partial \bar{u} / \partial y]$$

The last term on the right hand side of Equation (12) can be expressed as follows:

$$-\frac{\partial}{\partial y}(\overline{u'v'}) = +\frac{\partial}{\partial y}\left(\frac{\mu_t}{\rho}\frac{\partial \bar{u}}{\partial y}\right)$$

$$= \frac{\partial}{\partial y}\left(\nu_t \frac{\partial \bar{u}}{\partial y} \right)$$

Making this substitution Equation (12) then becomes

$$\frac{\partial}{\partial x}(\bar{u})^2 + \frac{\partial}{\partial y}(\bar{u}\bar{v}) = \nu \frac{\partial^2 \bar{u}}{\partial y^2} + \frac{\partial}{\partial y}\left(\nu_t \frac{\partial \bar{u}}{\partial y} \right)$$

or

$$\bar{u} \frac{\partial \bar{u}}{\partial y} + \bar{v} \frac{\partial \bar{u}}{\partial y} = \frac{\partial}{\partial y}\left[(\nu + \nu_t) \frac{\partial \bar{u}}{\partial y} \right] \qquad (13)$$

The boundary conditions for flow over a flat plate are

$$y = 0 \;:\; \bar{u} = \bar{v} = 0 \;;$$
$$y = \infty \;:\; \bar{u} = U_\infty .$$

Equation (13) is the basic equation to be used in this analysis. From this point on $\bar{u}$ will be replaced by u and $\bar{v}$ by v.

SIMILARITY SOLUTION

One of the significant results of the study is the reduction of Equation (13) from a partial differential equation to an ordinary differential equation by an affine substitution or similarity transformation. This is done by changing the variable x to ξ and y to η where

$$\eta = Ay/x^n \quad \text{and} \quad \xi = x \;,$$

where A and n are arbitrary constants to be chosen later. In potential flow the velocity u can be determined from the stream function ψ_p. That is,

$$u = \frac{\partial}{\partial y}\psi_p \quad \text{and} \quad v = -\frac{\partial \psi_p}{\partial x}$$

where

$$\psi_p = U_\infty y = U_\infty x^n \eta / A$$

It is now assumed that in the turbulent boundary layer that there exists a "stream function" ψ_t such that

$$\psi_t = U_\infty x^n f(\eta) / A$$

where $f(\eta)$ means some function of η and in the future will simply be replaced by f. Therefore, by analogy

$$u = \frac{\partial}{\partial y} \psi_t = U_\infty f'$$

and

$$v = -\frac{\partial}{\partial x} \psi_t = \frac{n U_\infty x^{n-1}}{A} (\eta f' - f)$$

where f' is $\partial (f) / \partial \eta$.

Hence the following relationships result:

$$\frac{\partial u}{\partial x} = -\frac{U_\infty f'' n \eta}{x}$$

$$\frac{\partial u}{\partial y} = \frac{U_\infty f'' A}{x^n}$$

$$\frac{\partial}{\partial y}\left[(\nu + \nu_t)\frac{\partial u}{\partial y}\right] = \nu \frac{U_\infty A^2 f'''}{x^{2n}} + \nu_t \frac{U_\infty A^2 f'''}{x^{2n}} + \frac{U_\infty f'' A^2}{x^{2n}} \frac{\partial(\nu_t)}{\partial \eta}$$

This, when substituted into Equation (13), results in the following:

$$-U_\infty n f'' f = (\nu + \nu_t) \frac{U_\infty A^2 f''}{x^{2n-1}} + \frac{U_\infty f'' A^2}{x^{2n-1}} \frac{\partial \nu_t}{\partial \eta} \qquad (14)$$

It is obvious from Equation (14) that n should be chosen such that n = 1/2. This, after rearrangement, results in the following:

$$-f''f = 2(1 + \nu_t/\nu) \frac{\nu A^2}{U_\infty} f''' + 2 \frac{\nu A^2 f''}{U_\infty} \frac{\partial (\nu_t/\nu)}{\partial \eta}$$

It follows that A should be chosen as

$$A^2 = U_\infty / \nu$$

If n = 1/2 and $A^2 = U_\infty/\nu$, Equation (14) becomes

$$-f''f = 2(1+\nu_t/\nu)f''' + 2f''\frac{\partial(\nu_t/\nu)}{\partial\eta} \qquad (15)$$

Equation (15) becomes a nonlinear ordinary differential equation with variable coefficients if it is assumed that $\nu_t = \nu_t(\eta)$ only. With this assumption it will be possible to obtain numerical results. For a particular value of x or a specified Re_x the assumption that $\nu_t = \nu_t(\eta)$ should be very good. For more details of the similarity solution see Appendix B.

The boundary conditions for the flow case in consideration are

$$f(0) = 0, \qquad f'(0) = 0, \qquad f'(\infty) = 1 \qquad (16)$$

As was mentioned previously, $f = f(\eta)$, $f' = \frac{\partial f}{\partial\eta}$, etc.
Also $\eta = y\sqrt{U_\infty x/\nu}$, and $f' = u/U_\infty$
It is interesting to note that Equation (15) becomes the solution to laminar flow over a flat plate when $\nu_t = 0$.
That is, Equation (15) becomes

$$-f''f = 2f''' \qquad (17)$$

which is commonly known as the Blasium solution to flow over a flat plate subject to the usual boundary conditions.

CHAPTER IV

NUMERICAL PROGRAM

One commonly used method to numerically solve ordinary differential equations is the method of Runge-Kutta [12]. However, such a method is really for initial-value problems, not boundary-value problems. Hence, the solution of a boundary-value problem with the Runge-Kutta method requires that an initial guess be made for the unknown boundary conditions at one end. The correct initial boundary condition guess results in the satisfaction of the boundary conditions at the other end. The Newton-Raphson method [13,14] reduces the method described from a trial and error art to a convenient numerical iteration.

Hence, in obtaining the numerical solution to Equation (15) with the boundary conditions given by Equation (16) a computer program was written which utilized both the Runge-Kutta method and the Newton-Raphson technique to obtain a solution. In particular, a fourth order Runge-Kutta method was used. For additional details on program used see Appendix C.

CHAPTER V

EFFECT OF VARIABLE COEFFICIENTS ON SIMILARITY SOLUTION

From Equation (15) it is seen that the numerical solution of that equation depends upon the values of the variable coefficients at any η. Hence, it is necessary to describe the ν_t/ν variation as a function of η.

Determination of Eddy Diffusivity

At this point it is of major interest to investigate the variance of the eddy diffusivity across the boundary layer. Now the eddy diffusivity can be evaluated in each of the regions of the turbulent boundary layer by application of the following:

$$\tau/\rho = (\nu_t + \nu)\, du/dy \tag{18}$$

where ν has the greatest effect near the wall and ν_t has an increasing effect in going toward the edge of the boundary layer. Equation (18) can be rearranged as follows:

$$1 + \nu_t/\nu = (\tau/\rho)/\nu \, \frac{du}{dy} = \frac{1}{\frac{du^+}{dy^+}}$$

$$\frac{\nu_t}{\nu} = \left[1/(du^+/dy^+)\right] - 1 \tag{19}$$

Now from Equation (5) for $y^+ < 5$

$$y^+ = u^+$$

then, using Equation (19), for $y^+ < 5$

$$\frac{\nu_t}{\nu} = \frac{1}{\frac{du^+}{dy^+}} - 1 = 0$$

Hence according to Marinelli's formulation

$$\frac{\nu_t}{\nu} = 0 \quad \text{up to} \quad y^+ = 5 \qquad (20)$$

Equation (5) also gives for $5 < y^+ < 30$

$$u^+ = -3.05 + 5.00 \ln y^+$$

which when put into Equation (19) gives

$$\frac{\nu_t}{\nu} = \frac{1}{\frac{d(5 \ln y^+)}{dy^+}} - 1 = \frac{y^+}{5} - 1 \qquad (21)$$

which is a simple linear variation. Equation (5) for $y^+ > 30$ also yields a similar variation.

The idea that ν_t goes to zero at some arbitrary distance from the wall such as $y^+ = 5$ is an oversimplification. Deissler proposed that ν_t only approaches zero as y^+ approaches zero. Application of Equation (19) to Equation (6) given by Deissler gives

$$\frac{\nu_t}{\nu} = 0.6119\, u^+ y^+ \qquad (22)$$

Van Driest [8] proposed that the wall has a dampening effect on the variation which Deissler [7] used to obtain the following

$$\frac{\nu_t}{\nu} = 0.0154\, u^+ y^+ [1 - \exp(-0.0154\, u^+ y^+)] \qquad (23)$$

which has been used very successfully in some heat transfer calculations referred to in Kays [14]. Spalding also takes this exponential dampening into account as can be seen from Equation (7) and Equation (19) which gives

$$\frac{\nu_t}{\nu} = \frac{0.4}{9.025}\left[e^{.4u^+} - 1 - ku^+ + \frac{(ku^+)^2}{2!} - \frac{(ku^+)^3}{3}\right] \qquad (24)$$

Model of Eddy Diffusivity

If ν_ϵ/ν is equal to zero for all η it would be expected that the numerical solution obtained would be the same as the one obtained for the Blasius profile. When this ν_ϵ/ν variation was used the results obtained compared exactly with the results given by Schlichting [10] for the Blasius solution.

To examine the effect on the solution several different variations of ν_ϵ/ν versus η were tried and compared with a standard curve.

The general type of model of ν_ϵ/ν versus η that was used is shown in Figure 3.

Examination of Equation (15) shows that the two values of interest for the variable coefficients are ν_ϵ/ν and $\frac{\partial}{\partial \eta}(\nu_\epsilon/\nu)$ at any η. The simple model of variation of ν_ϵ/ν versus η shown in Figure 3 will provide a means of determining the effects of both coefficients of Equation (15).

Several figures are included in what follows to show the effect of the ν_ϵ/ν variation on the numerical solution to Equation (15). Reference to Figure 4 will clarify the general technique to be used. In Figure 4, the graph on $\nu_\epsilon/\nu, \eta$ coordinates represents the input variation and the graph on f', η coordinates represents the effect on the numerical solution of Equation (15). For example, the curve marked by A on $\frac{\nu_\epsilon}{\nu}, \eta$ coordinates corresponds to the curve on f', η coordinates. The reason for presenting the results of this study in the general form shown in Figure 4 is for clarification of the effects of the variation of ν_ϵ/ν versus η on the solution of Equation (15).

To obtain the solution of Equation (15), the point where the

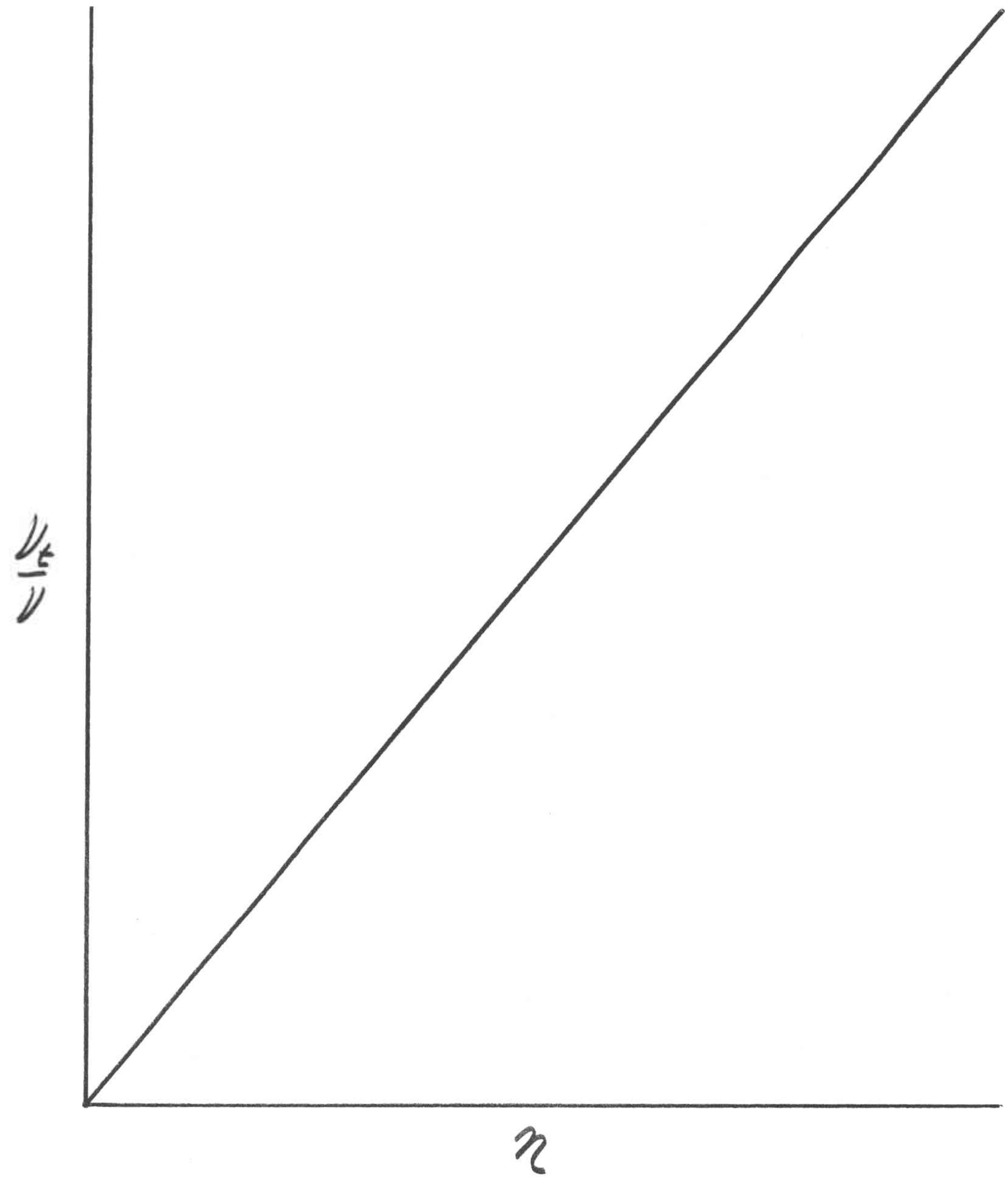

Fig. 3. -- Linear ν_t/ν variation as a function of η .

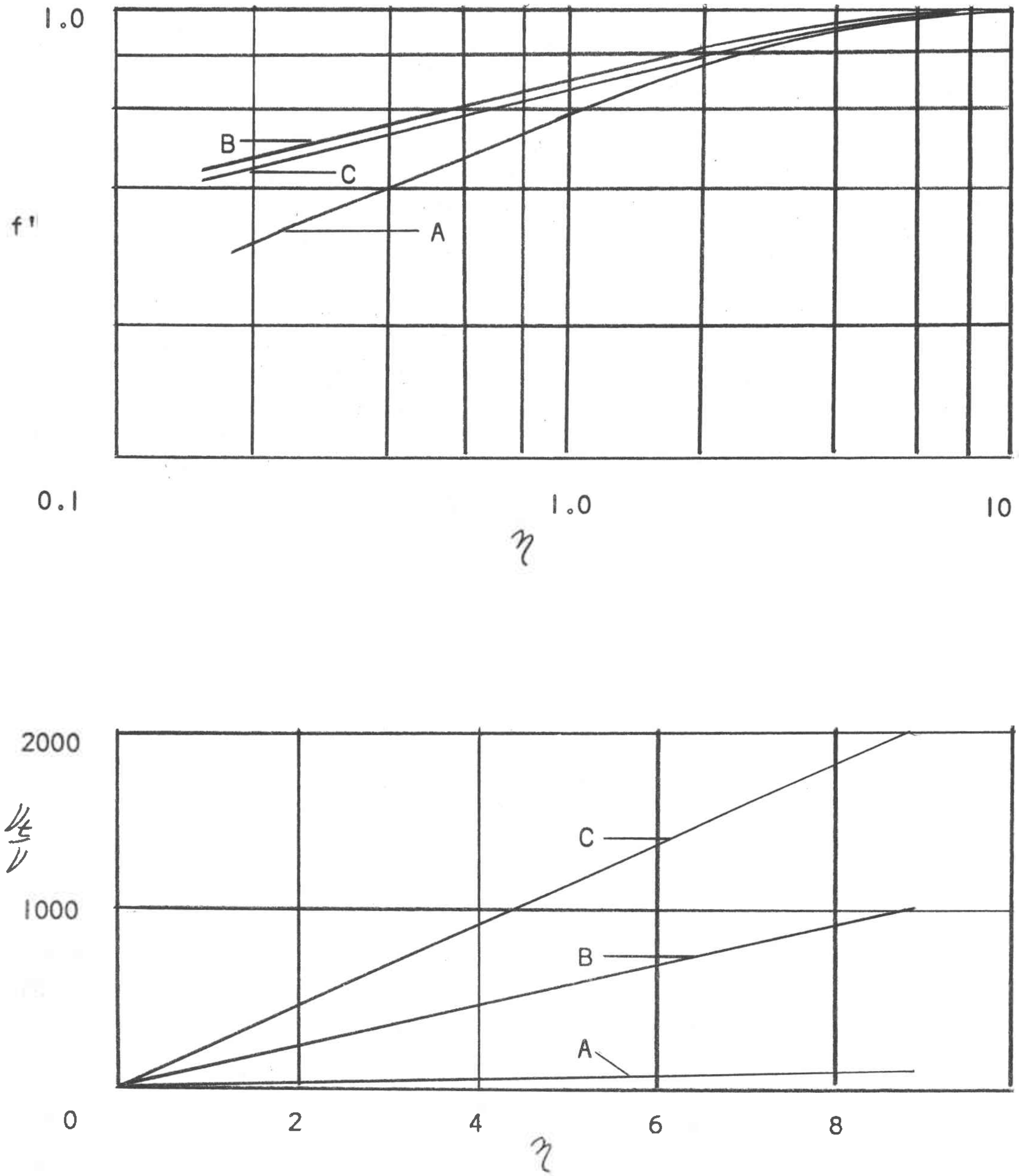

Fig. 4. -- Input variation and effect on numerical solution.

boundary layer ceases to exist must be specified. For instance, in a boundary layer that is completely laminar $f'(\infty) = f'(5)$. The numerical solution to Equation (15) is then forced to have the value of $f' = 1.0$ at $\eta = 5.0$.

Figure 4 shows the effect on the turbulent boundary-layer equation of three different ramp inputs when $\eta = \infty$ is specified as $\eta = 8.8$. Input A gives the term $\frac{\partial(\nu_t/\nu)}{\partial\eta}$ a value of about 11.3 while input B gives the slope a value of 113 and input C gives the slope a value of 226. The results plotted show that as the slope is increased from 11.3 to 113 the solution curve is raised but that somewhere between a slope of 113 and 226 the curve reaches a maximum and starts to decrease. Additional numerical data determined that the slope for which a maximum was reached was about 133. The value of ν_t/ν at any η is quite a bit different for each input. From Figure 4 it is seen that the solution curve increases as the value of ν_t/ν increases up to a point and then decreases. From Figure 4 it is not clear which term, that is $\frac{\partial(\nu_t/\nu)}{\partial\eta}$ or ν_t/ν is really controlling the solution. However, examination of the numerical values, term for term, in the similarity solution determined that the slope has a much greater effect than the value of ν_t/ν at any η. This will be shown later in the thesis.

CHAPTER VI

CHANGE OF COORDINATES

The results obtained for turbulent flow in this study are compared with a plot of Spalding's representation of experimental data. Spalding's representation was used because of its convenient form. It seems to be generally agreed that this curve adequately fits the data, at least within the experimental scatter. The only problem in using this curve fit is that it is in terms of u^+ and y^+ instead of f' and η. It can, however, be shown that (see Appendix A)

$$\eta = (y^+) \sqrt{\frac{2}{C_f}} \frac{1}{\sqrt{Re_x}} \tag{25}$$

and

$$f' = (u^+) \sqrt{\frac{C_f}{2}} \tag{26}$$

Hence, all that is necessary to convert u^+, y^+ data to f', η points is to know the relationship between C_f and Re_x at any particular Re_x. One such relationship that has been shown to be valid for turbulent flow over a flat plate was given by Schultz and Grunow [15]. The relationship is

$$C_f = 0.370 \left(\log_{10} Re_x \right)^{-2.58} \tag{27}$$

A comparison of Equation (27) with experimental data [16] is shown on Figure 5, which shows the relationship to be in good agreement with experimental data.

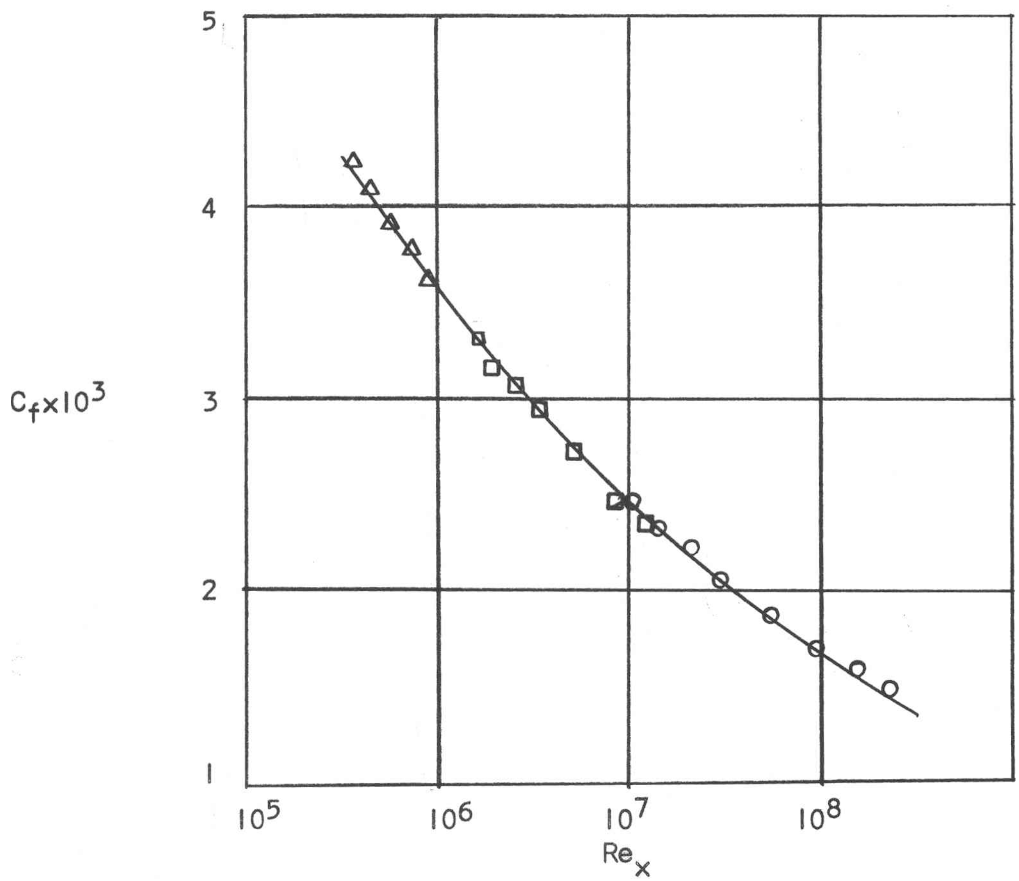

Fig. 5. -- Local skin coefficient for smooth wall, zero pressure gradient. Experimental values represented by points. The curve is Equation (27). (After Schubauer and Tchen [16])

Using Equations (25), (26), (27), it is easy to convert Spalding's representation from u^+, y^+ coordinates to f', η coordinates for any value of Re_x.

CHAPTER VII

COMPARISON OF SIMILARITY SOLUTION TO EXPERIMENTAL DATA

For flow over a flat plate with zero pressure gradient it has been found experimentally [10] that it can generally be assumed that transition from laminar to turbulent flow will take place in the range of $Re_x = 3.5 \times 10^5$ to $Re_x = 10^6$. In this analysis it will be assumed that turbulent flow exists at $Re_x = 5 \times 10^5$.

Figure 6 shows flow profiles for various Re_x and the Blasius profile. All the curves except the Blasius profile are Spalding's u^+, y^+ representation transformed to f', coordinates. The relationship between the curves with respect to the increasing Re_x is very interesting. It shows that as the Re_x increases, the major part of the velocity change moves closer to the wall. From this point on all curves will be for a $Re_x = 10^6$.

Figure 7 shows the effect of the inputs shown on Figure 8 on the solution. As may be seen, the slope of the u_ϵ/U versus η increases, and the curve moves up to a certain value and then decreases. As before, the slope at which the maximum occurred, that is the slope at which the solution curve attained its highest value, was found to be about 133.

Clauser [17], as well as several others, has suggested that the viscous sublayer of a turbulent boundary layer is about 1/1000 to

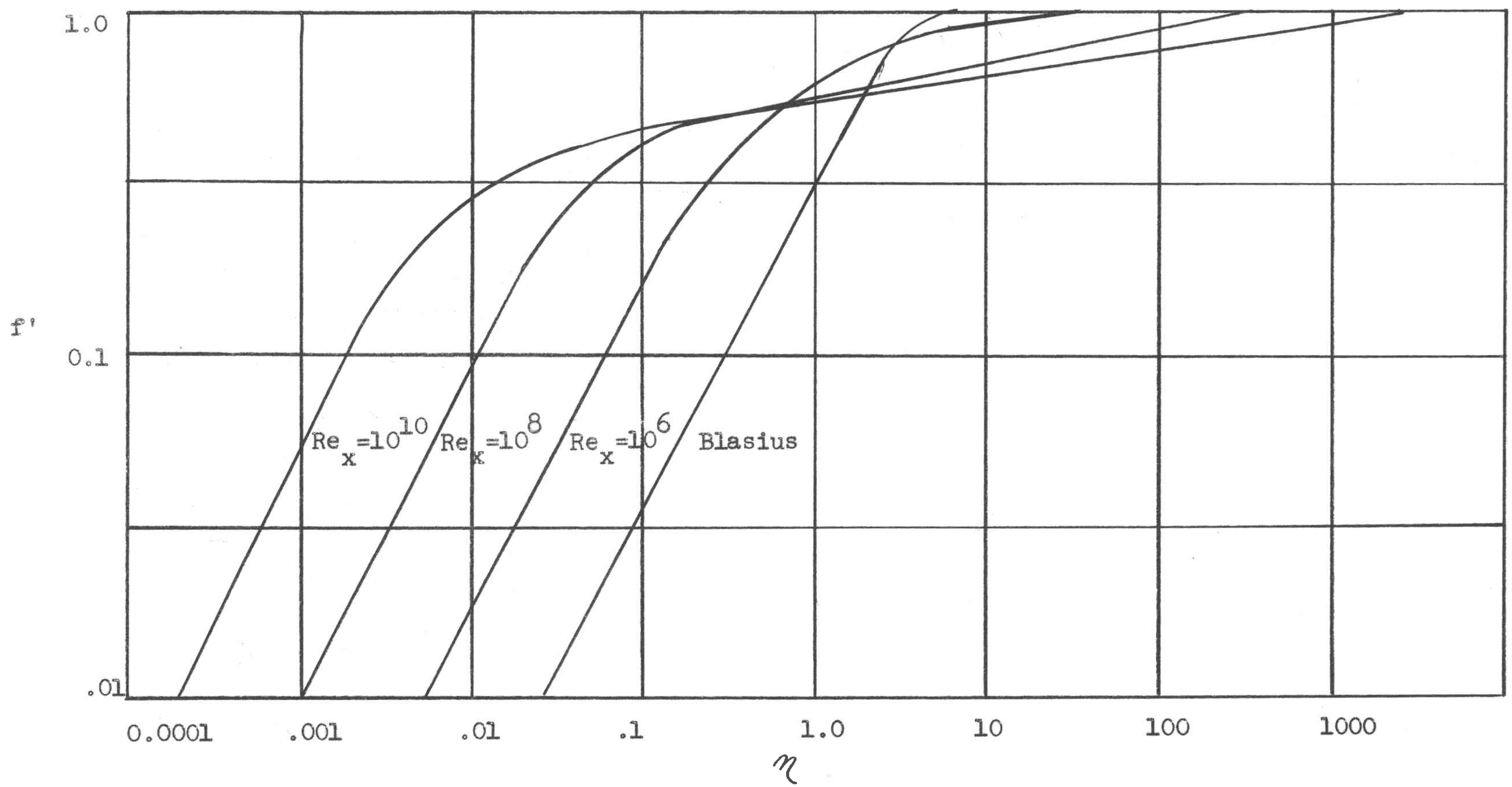

Fig. 6. -- Spalding's u^+, y^+ correlation on f', η coordinates for various Re_x.

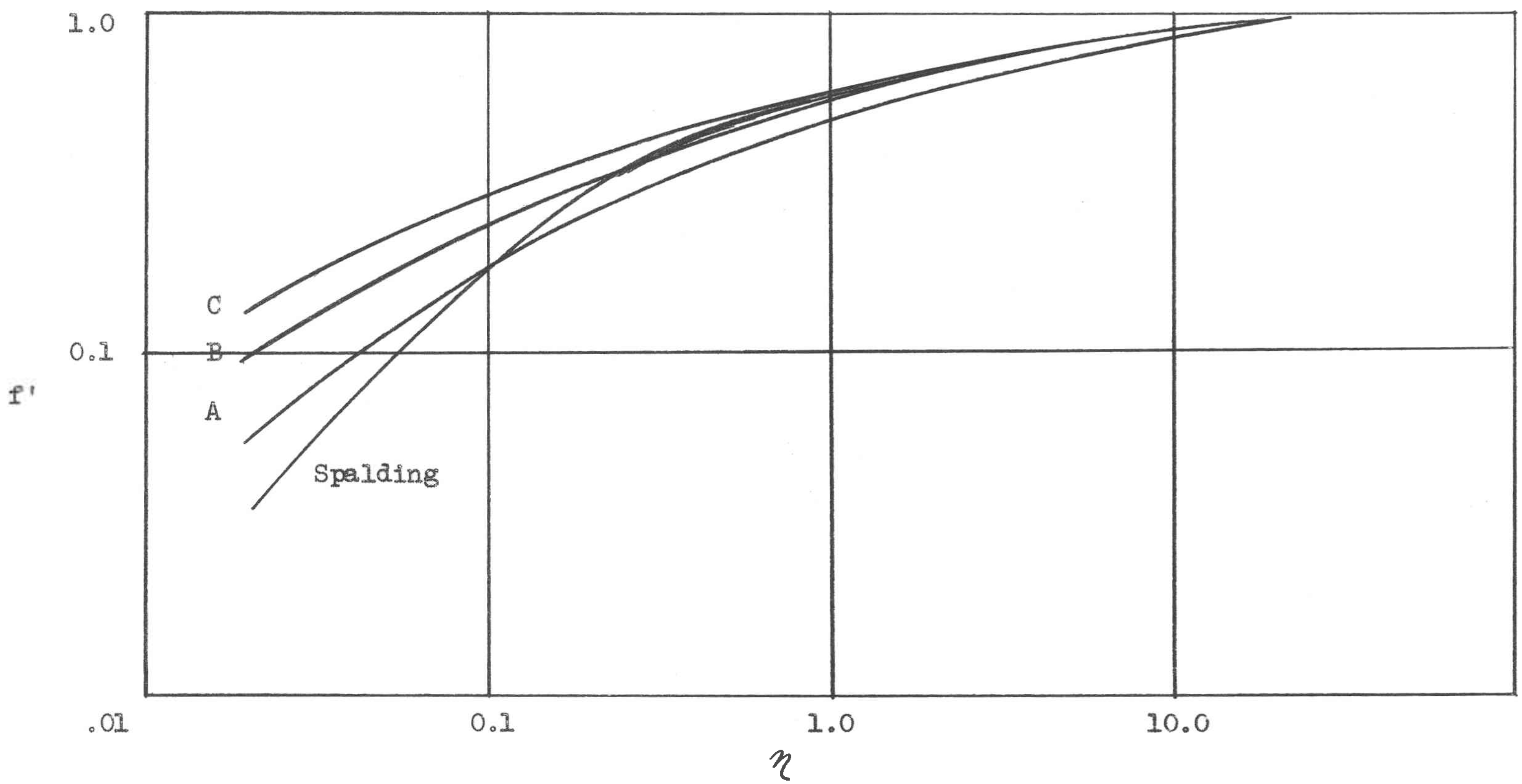

Fig. 7. -- Input variation effect of Figure 8 on numerical solution.

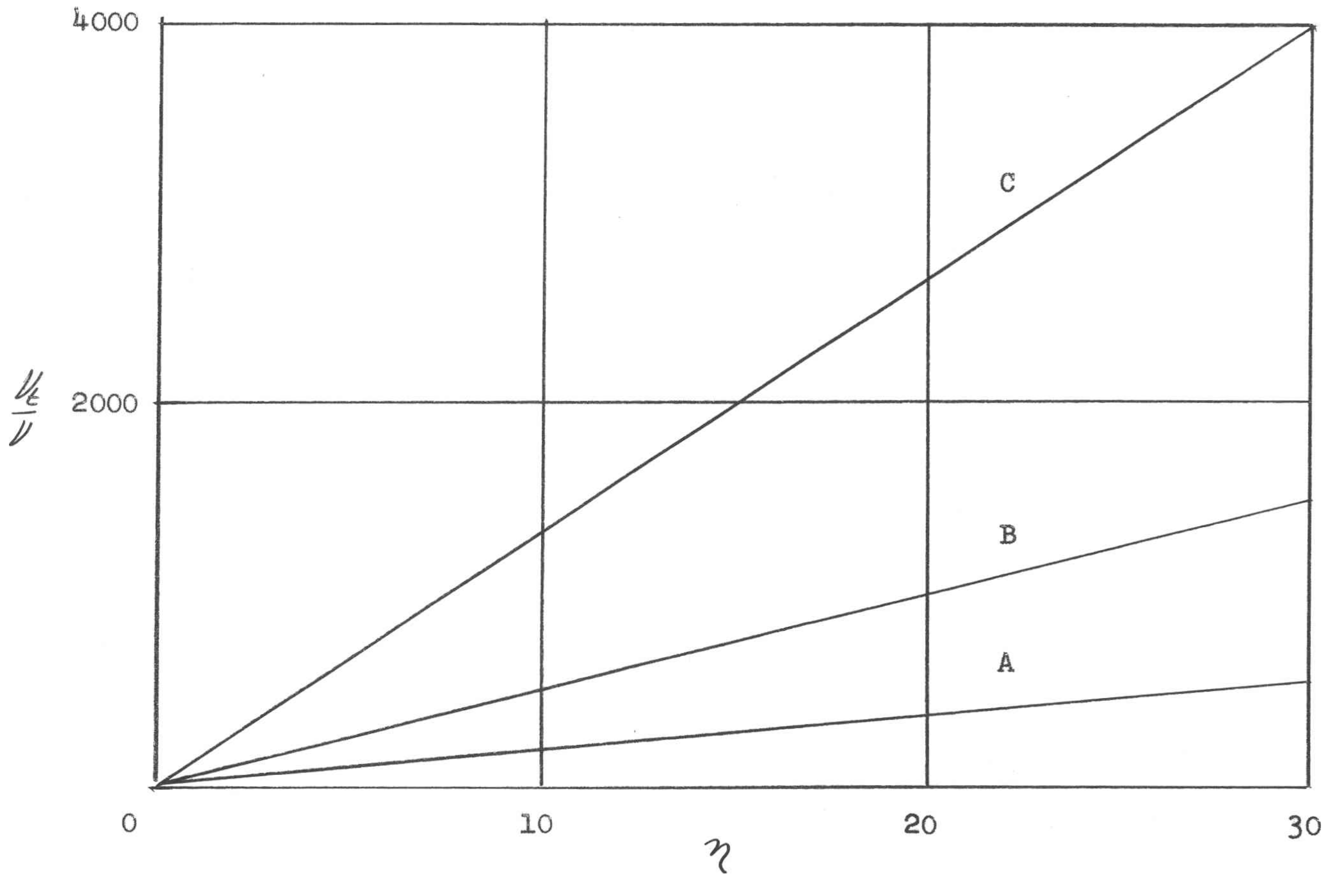

Fig. 8. -- Input variation used to obtain Figure 7.

1/100 of the total thickness of the boundary layer. This suggests that the variation of ν_t/ν versus η shown on Figure 9 might yield interesting results. In other words, it seems reasonable to think, at least for a simple model, that $\nu_t = 0$ in the viscous sublayer. The effect of such an offset is shown on Figure 10 where Figure 11 shows the input variation. It should be pointed out that Figure 11 is no longer to scale. As shown, the result is to bend the solution curve in the correct direction. In fact, the influence of a very small offset seems to be very critical.

Equation (20) suggested that $\nu_t = 0$ up to a value of about $y^+ = 5$ and Equation (21) suggested that the variation is linear after $y^+ = 5$. Choosing a value of $\eta \approx$ ($y^+ = 5$) as the offset point, and using a ramp input that would yield the curve with the maximum height, the results shown in Figure 12 were obtained where Figure 13 illustrates the input variation. Also plotted on Figure 12 are the curve fits of Spalding [9] and Diessler [7]. It is very interesting to notice that the agreement with Curve B is excellent near the wall and near the edge of the boundary layer but that in the middle the agreement is not as good.

At this point it is clear that the offset has a large influence on the solution curve. Previously it has been shown that the combination of slope and value of ν_t/ν also have a large effect. To determine which of the last two variations had the greatest effect, the solution curves for Figure 14 were found. All three inputs, except for a small region, have the same value of slope but considerably different values of ν_t/ν. The solution curves were not plotted because

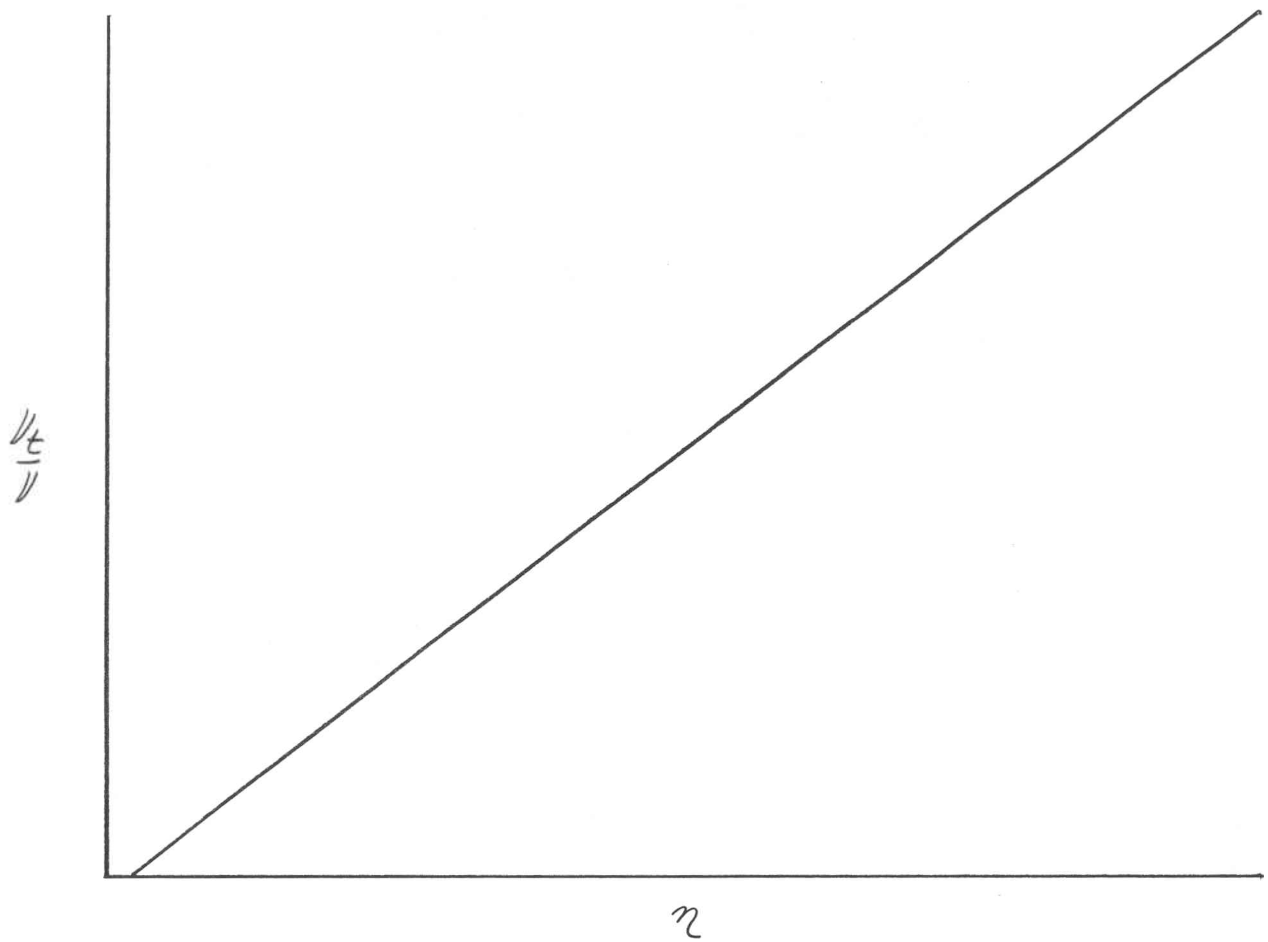

Fig. 9. -- Improved model of ν_t/ν vs. η .

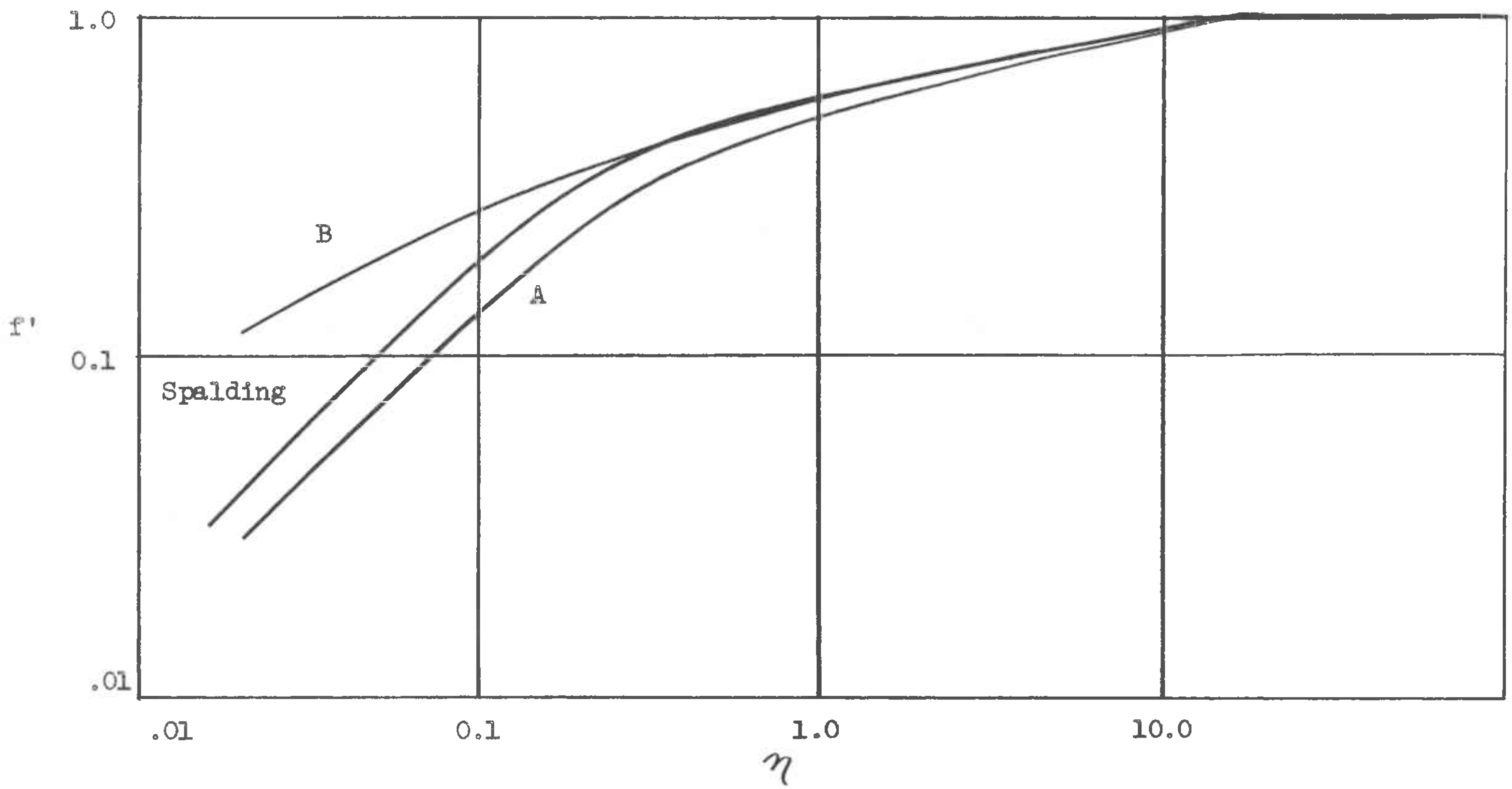

Fig. 10. -- Input variation effect of Figure 11 on numerical solution.

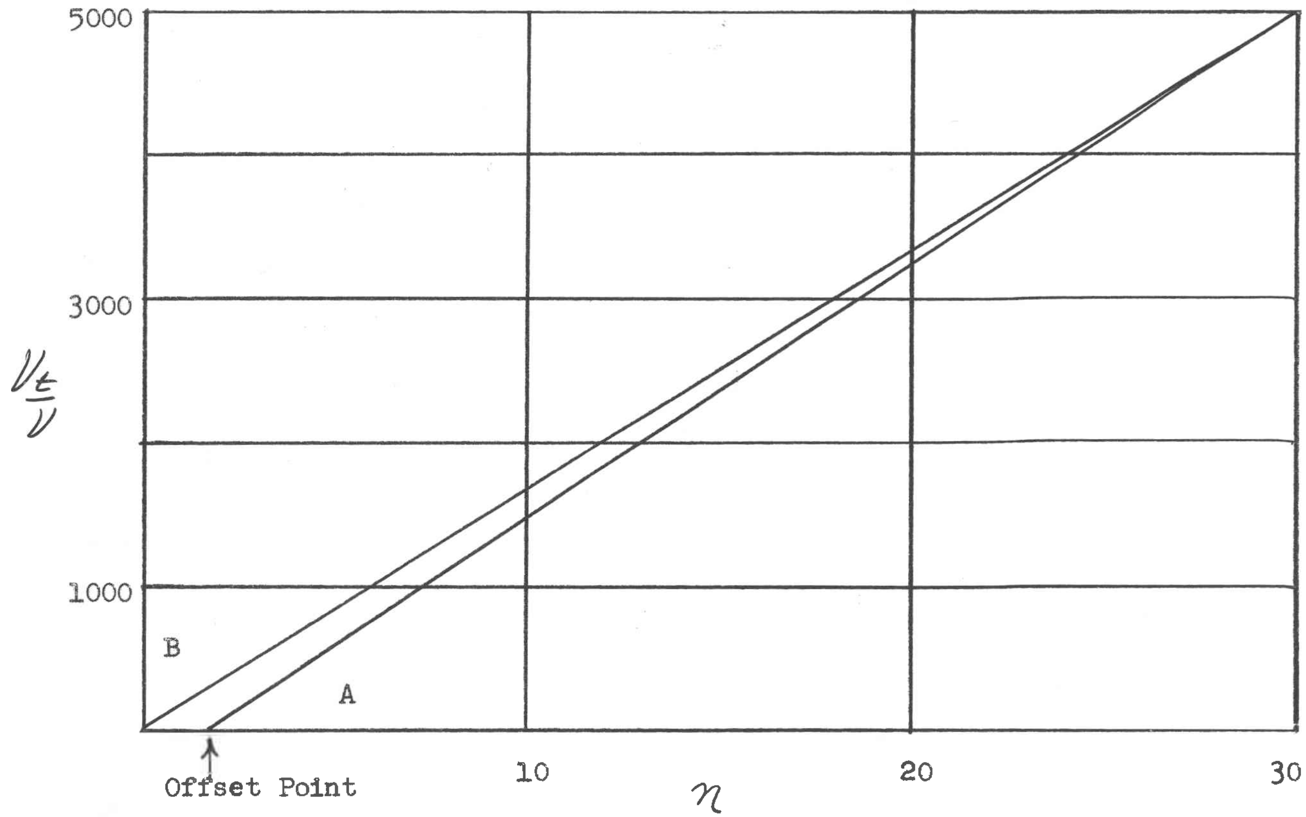

Fig. 11. -- Input variation used to obtain Figure 10. Offset point (η = 0.1) not to scale.

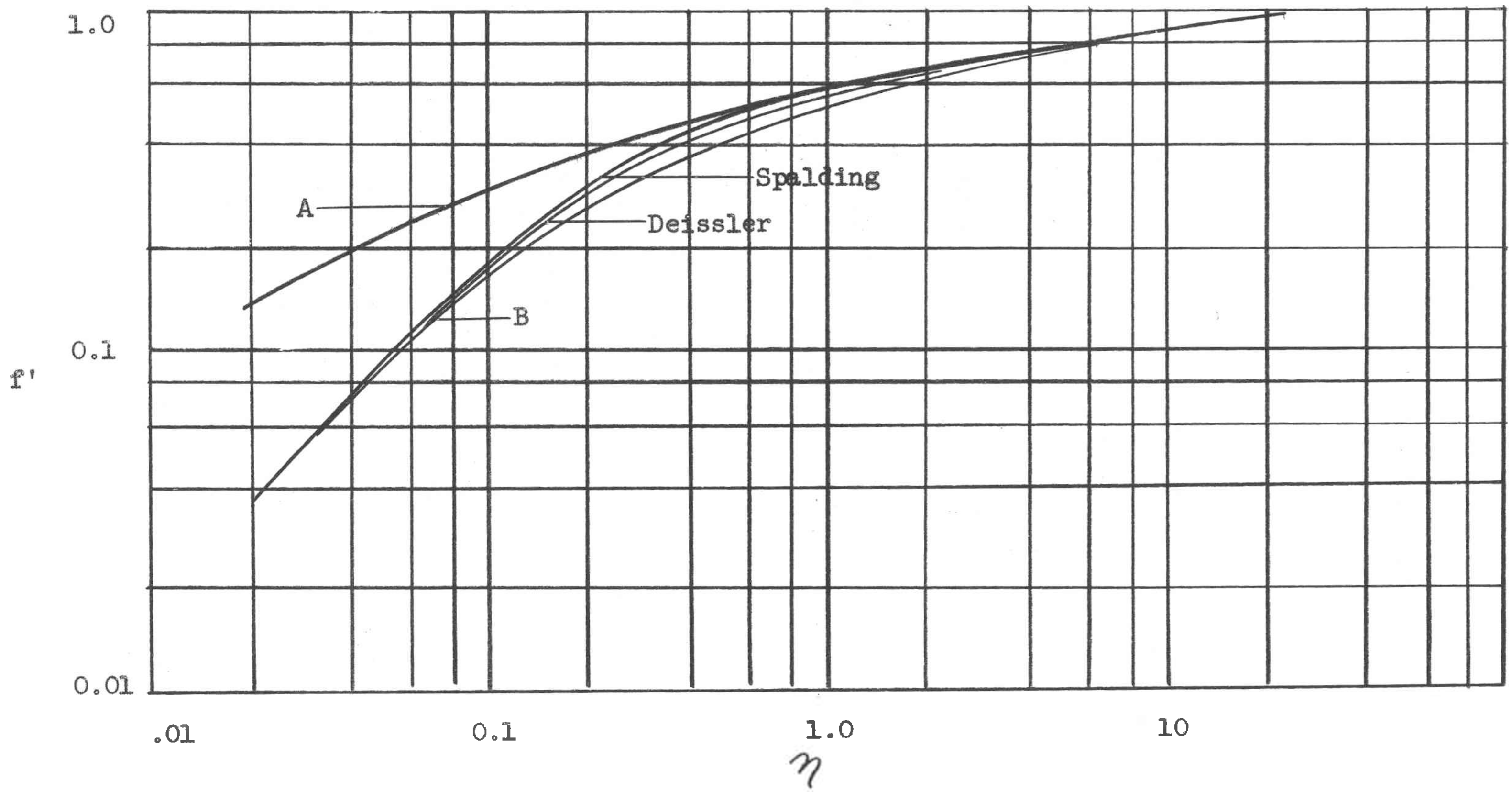

Fig. 12. -- Input variation effect of Figure 13 on numerical solution.

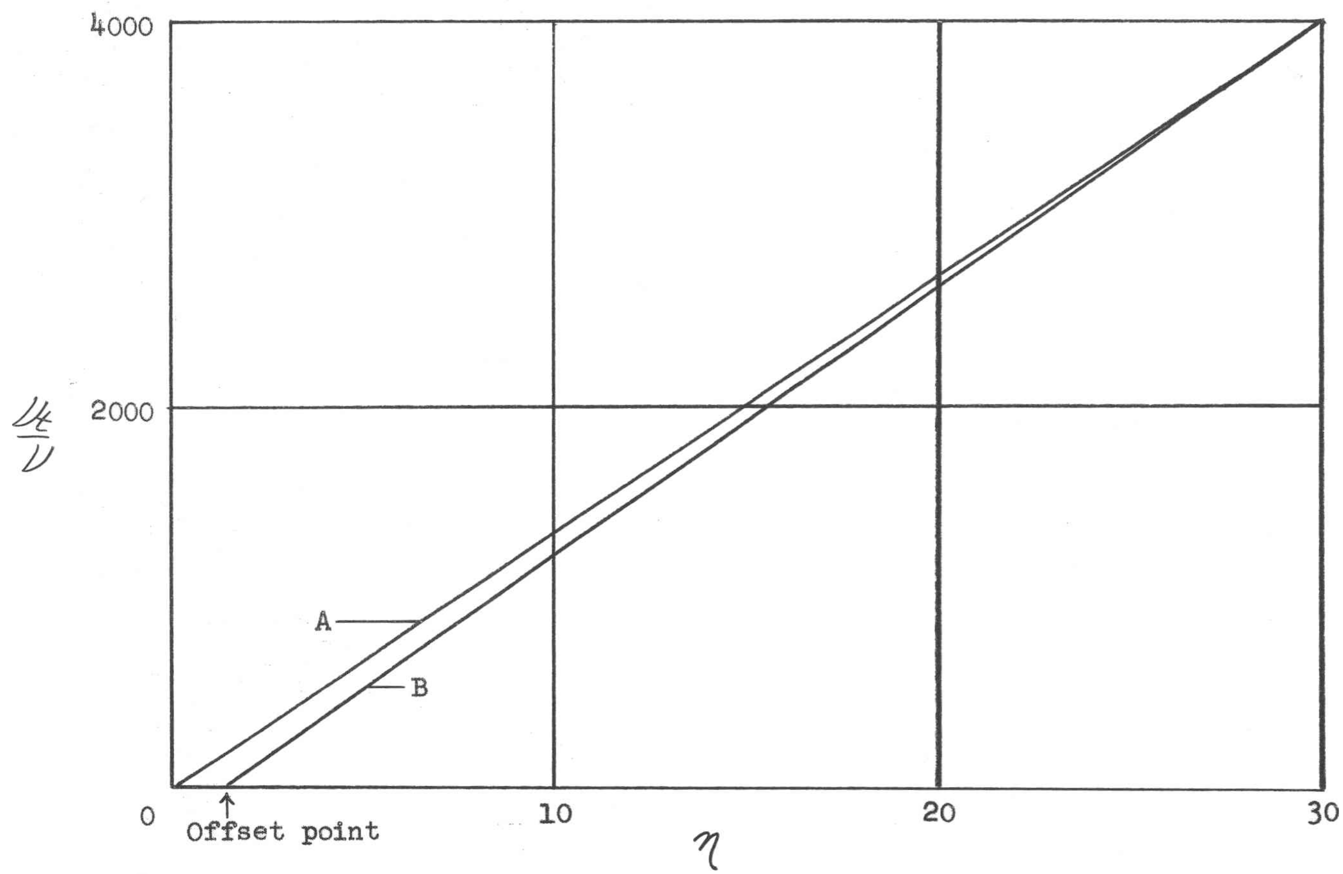

Fig. 13. -- Input variation used to obtain Figure 12. Offset point ($\eta = 0.07$) not to scale.

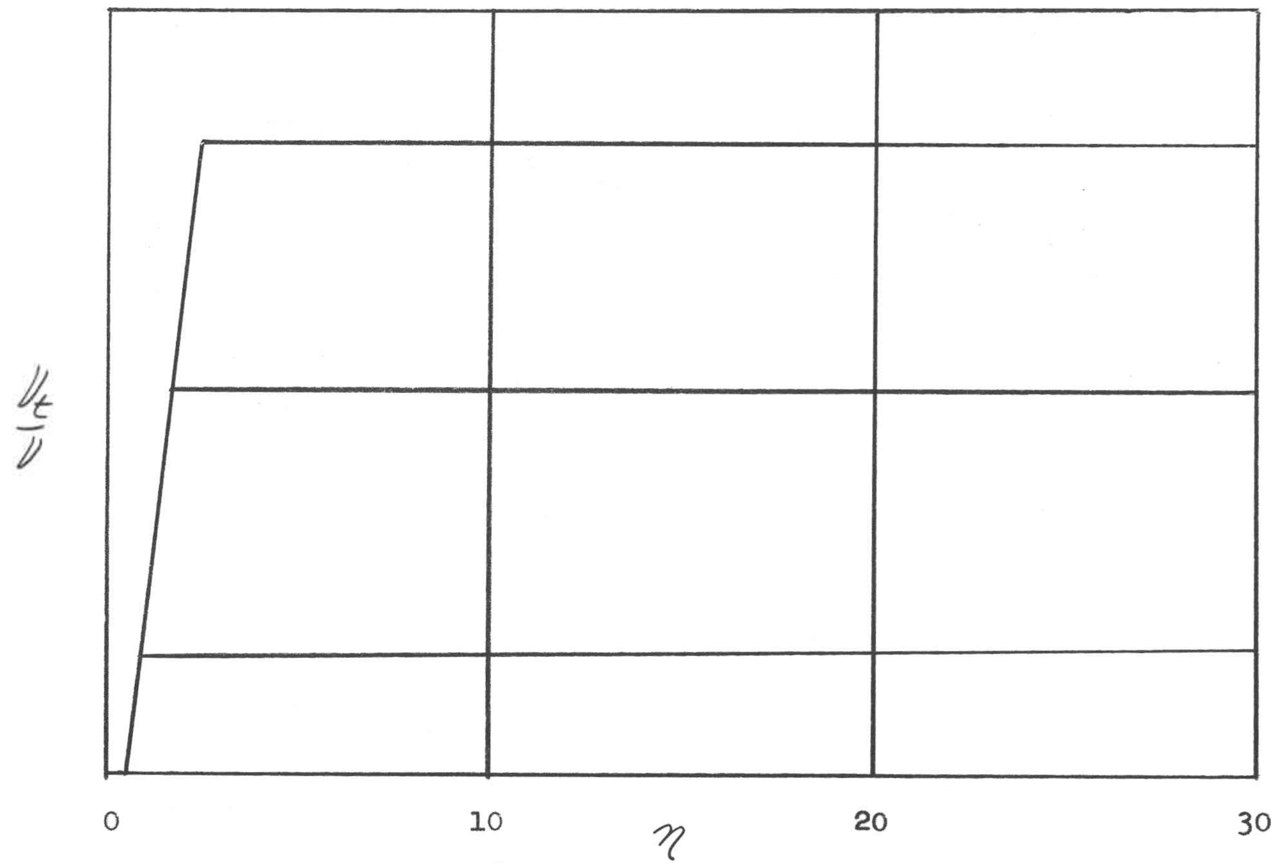

Fig. 14. -- Additional Input Variations.

they all fell upon one another. This suggests that the slope has a much greater effect than the value of u_+/u.

It was also noted that any of the solution curves obtained from the input of Figure 14 fell on Curve B of Figure 12 which suggests that the slope has its greatest effect near the offset point.

Figure 12 shows that the simple model for the variation of u_+/u versus η was not completely successful in duplicating either Spalding's or Deissler's representation of the data. Figure 15 shows the same curves on u^+, y^+ coordinates, where the lack of agreement is more obvious.

To obtain meaningful results it was necessary to use a step size that was small enough in magnitude so that the behavior near the wall could be determined. For $Re_x = 10^6$ the step size used was $\Delta\eta = 0.02$.

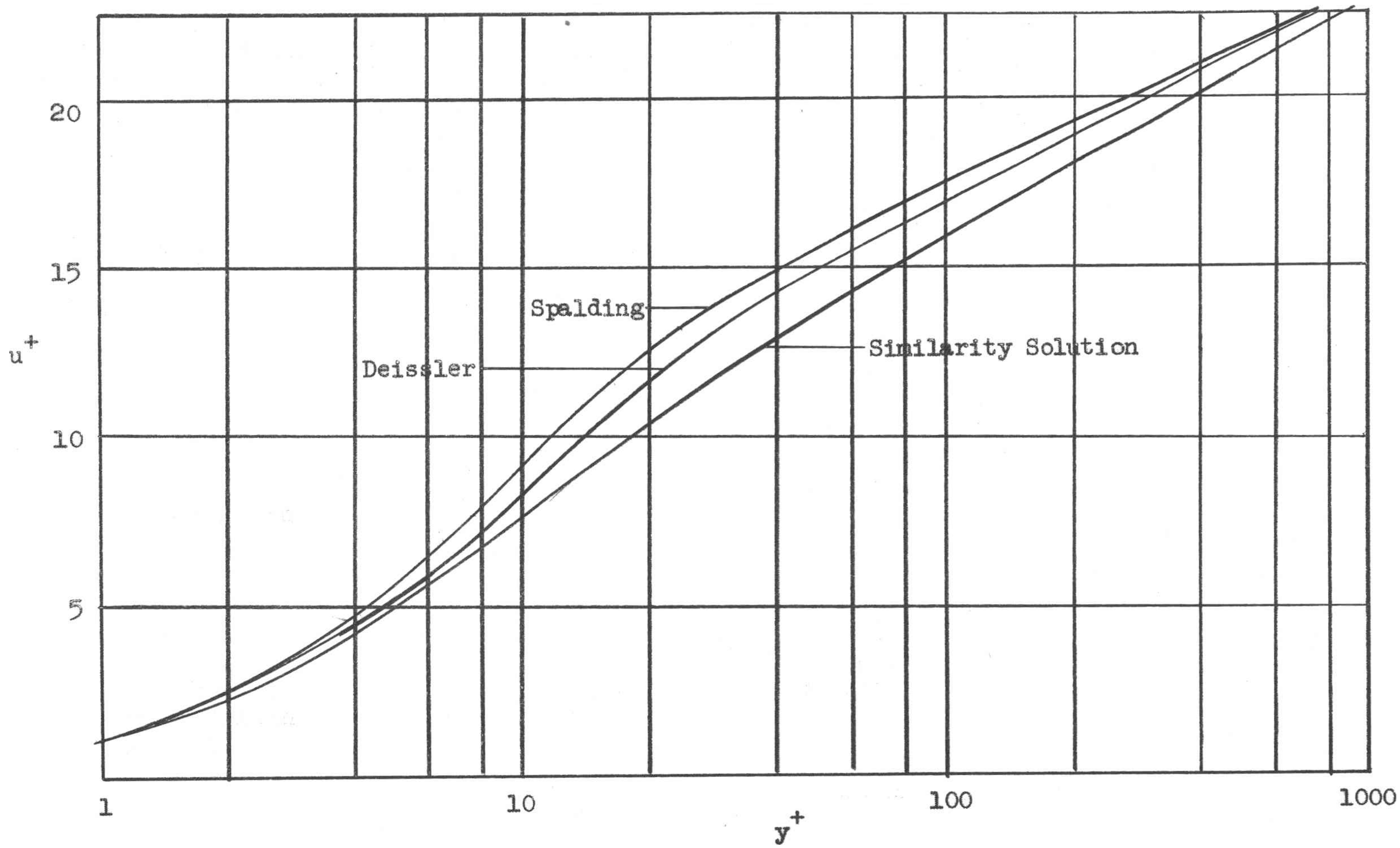

Fig. 15. -- Comparison of similarity solution with Spalding's and Deissler's representations.

CHAPTER VIII

DISCUSSION OF RESULTS

The model used to obtain the results reported was based on Equation (20) and Equation (21). As explained in Chapter IV, this is an oversimplification of the actual variation. It seems reasonable to assume that if a more realistic model of the eddy diffusivity variation had been used that better results would have been obtained. Figure 16 shows the variation that has been proposed by Spalding and the variation used in this thesis. The comparison suggests that the next model to be used should have a general form of the Spalding representation.

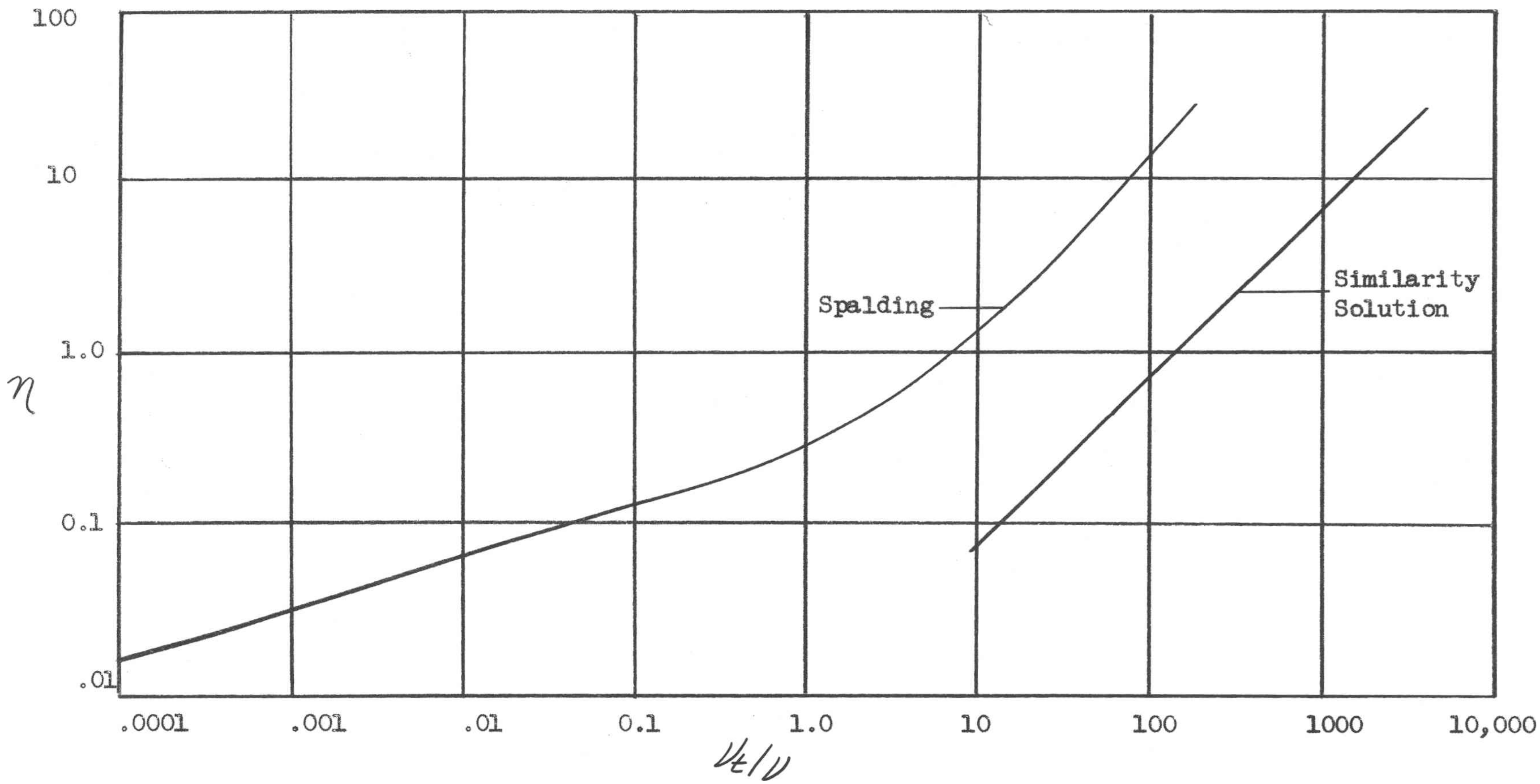

Fig. 16. -- Comparison of eddy diffusivity model used with Spalding's suggested model.

CHAPTER IX

CONCLUSIONS AND RECOMMENDATIONS

The results obtained suggest that it will be possible to obtain a simple model for the variation of the eddy diffusivity which will yield a velocity profile that is in agreement with experimental results. When the working model of the variation is obtained it can be used in other applications to predict velocity and temperature profiles.

The similarity solution obtained is not a true similarity solution. A family of curves dependent on Re_x are obtained instead of one universal curve, as is the case in the Blasius similarity solution.

For the diffusivity model tested the two parameters that seemed to have the greatest effect on the solution were the offset point and value of the slope near the offset point. The results also illustrated that there was the optimal value for the slope of about 133.

It is recommended that the general type of variation shown in Figure 16 be used as the next step in obtaining the desired model.

The numerical method used to obtain the above solutions employs a constant step size procedure. This introduces two problems. The first problem can be easily understood by examination of Figure 6. For a $Re_x = 10^6$ a step size of at least $\Delta\eta = 0.02$ must be used to obtain a part of the linear portion of the curve. However, for $Re_x = 10^8$ the step size must be reduced to at least $\Delta\eta = 0.002$. For a step size of $\Delta\eta$ = 0.02 the time required for execution is about three minutes per solution while for a $\Delta\eta$ = 0.002 the time required is in excess of one hour. Hence, it is suggested that the computer program be rewritten to include a variable step size such that it is very small when $\eta \approx 0$ and $\Delta\eta$ increases in size as the value of η approaches the edge of the boundary layer. The second problem introduced by the constant step size is that it is not economical to let the solution seek its own asymptotic value of f'. Hence the present program requires convergence to f' = 1.0 at some specified . A variable step size program will greatly reduce the computational time required per run. With this added flexibility, the numerical integration can be expected to seek its natural asymptote, based upon initial slope (f''(0)) and diffusivity profile. This will allow the determination of an acceptable $\nu_t(\eta)$ profile without prior information on the boundary layer thickness.

Appendix A

Change of Coordinates

Now, $y^+ = \frac{y}{\nu}\sqrt{\frac{\tau_w}{\rho}}$ and $\eta = y\sqrt{\frac{U_\infty}{\nu x}}$

Also $c_f = \frac{\tau_w}{\frac{1}{2}\rho U_\infty^2}$, hence $\sqrt{\frac{\tau_w}{\rho}} = \sqrt{\frac{c_f U_\infty^2}{2}}$

Which gives

$$\eta = y\sqrt{\frac{U_\infty}{\nu x}} = \frac{y}{\nu}\sqrt{\frac{\tau_w}{\rho}}\left(\sqrt{\frac{\rho}{\tau_w}}\,\nu\sqrt{\frac{U_\infty}{\nu x}}\right)$$

$$= y^+\sqrt{\frac{2}{c_f}}\sqrt{\frac{\nu}{x U_\infty}}$$

$$= y^+\sqrt{\frac{2}{c_f}}\frac{1}{\sqrt{Re_x}}$$

Also, $u^+ = u\sqrt{\frac{\tau_w}{\rho}}$ and $f' = u/U_\infty$

Therefore

$$f' = \frac{u}{U_\infty} = \left(u\sqrt{\frac{\rho}{\tau_w}}\right)\left(\sqrt{\frac{\tau_w}{\rho}}\frac{1}{U_\infty}\right)$$

$$= u^+\sqrt{\frac{\tau_w}{\rho}}\frac{1}{U_\infty}$$

$$= u^+\sqrt{\frac{c_f}{2}}$$

APPENDIX B

SIMILARITY SOLUTION

THE GOVERNING EQUATIONS ARE CONTINUITY

$$\frac{\partial u}{\partial x} + \frac{\partial v}{\partial y} = 0$$

AND MOMENTUM

$$u\frac{\partial u}{\partial x} + v\frac{\partial u}{\partial y} = \frac{\partial}{\partial y}\left[(\nu + \nu_t)\frac{\partial u}{\partial y}\right]$$

NOW CHANGE THE VARIABLES SUCH THAT

$x \rightarrow \xi$ AND $y \rightarrow \eta$ where

$$\eta = \frac{Ay}{x^n} \quad \text{OR} \quad y = \frac{x^n \eta}{A}$$

ALSO ASSUME $\psi_t = \dfrac{U_\infty x^n f(\eta)}{A}$

NOW SINCE $u = \dfrac{\partial \psi}{\partial y}$ AND $v = -\dfrac{\partial \psi}{\partial x}$

THE FOLLOWING ARE OBTAINED

$$\frac{\partial \eta}{\partial x} = -n A y x^{-(n+1)} = -\frac{n\eta}{x}$$

$$\frac{\partial \eta}{\partial y} = \frac{A}{x^n}$$

$$\frac{\partial \psi_t}{\partial \eta} = \frac{U_\infty x^n f'}{A}$$

$$\frac{\partial \psi_t}{\partial \xi} = \frac{U_\infty f n x^{n-1}}{A}$$

TRANSFORMING THE COORDINATES GIVES

$$d\psi_t = \frac{\partial \psi}{\partial \xi} d\xi + \frac{\partial \psi}{\partial \eta} d\eta$$

$$u = \frac{\partial \psi}{\partial y} = \frac{\partial \psi}{\partial \xi}\frac{\partial \xi}{\partial y} + \frac{\partial \psi}{\partial \eta}\frac{\partial \eta}{\partial y} = \frac{U_\infty x^n f' A}{A x^n} = U_\infty f'$$

OR $f' = u/U_\infty$

$$v = \frac{\partial \psi}{\partial x} = \frac{\partial \psi}{\partial \xi}\frac{\partial \xi}{\partial x} + \frac{\partial \psi}{\partial \eta}\frac{\partial \eta}{\partial x} = \frac{-n U_\infty f x^{n-1}}{A} + \frac{U_\infty x^n f'}{A}\left(-\frac{n\eta}{x}\right)$$

$$= \frac{n U_\infty x^{n-1}}{A}(\eta f' - f)$$

$$\frac{\partial u}{\partial x} = \frac{\partial u}{\partial \eta}\frac{\partial \eta}{\partial x} + \cancel{\frac{\partial u}{\partial \xi}}^{\,0}\frac{\partial \xi}{\partial x} = -\frac{U_\infty f'' n \eta}{x}$$

$$\frac{\partial u}{\partial y} = \frac{\partial u}{\partial \eta}\frac{\partial \eta}{\partial x} + \cancel{\frac{\partial u}{\partial \xi}}^{\,0}\frac{\partial \xi}{\partial x} = \frac{U_\infty f'' A}{x^n}$$

$$\frac{\partial}{\partial y}\left[(\nu + \nu_t)\frac{\partial u}{\partial y}\right] = \frac{\partial}{\partial y}\nu\frac{\partial u}{\partial y} + \frac{\partial}{\partial y}\left(\nu_t \frac{\partial u}{\partial y}\right)$$

$$= \nu\frac{\partial^2 u}{\partial y^2} + \nu_t\frac{\partial^2 u}{\partial y^2} + \frac{\partial u}{\partial y}\frac{\partial \nu_t}{\partial y}$$

where

$$\frac{\partial^2 u}{\partial y^2} = \frac{\partial}{\partial \xi}\left(\frac{U_\infty f'' A}{x^n}\right)\cancel{\frac{\partial \xi}{\partial y}}^{\,0} + \frac{\partial}{\partial \eta}\left(\frac{U_\infty f'' A}{x^n}\right)\frac{\partial \eta}{\partial y}$$

$$= \frac{U_\infty A^2 f'''}{x^{2n}}$$

$$\frac{\partial \nu_t}{\partial y} = \frac{\partial \nu_t}{\partial \xi}\cancel{\frac{\partial \xi}{\partial y}}^{\,0} + \frac{\partial \nu_t}{\partial \eta}\frac{\partial \eta}{\partial y} = \frac{A}{x^n}\frac{\partial \nu_t}{\partial \eta}$$

HENCE

$$\frac{\partial}{\partial y}\left((\nu_t + \nu)\frac{\partial u}{\partial y}\right) = \nu\frac{U_\infty A^2 f'''}{x^{2n}} + \nu_t\frac{U_\infty A^2 f'''}{x^{2n}} + \frac{U_\infty f'' A^2}{x^{2n}}\frac{\partial \nu_t}{\partial \eta}$$

Which gives the following for the momentum

equation

$$-\frac{U_\infty f' U_\infty f'' n\eta}{x} + \frac{n U_\infty x^{n-1}}{A}(\eta f' - f)\frac{U_\infty f'' A}{x^n} =$$

$$\nu \frac{U_\infty A^2 f'''}{x^{2n}} + \nu_t \frac{U_\infty A^2 f'''}{x^{2n}} + \frac{U_\infty f'' A^2}{x^{2n}} \frac{\partial \nu_t}{\partial \eta}$$

WHICH REDUCES TO

$$-U_\infty^2 n f'' f = (\nu + \nu_t)\frac{U_\infty A^2 f'''}{x^{2n-1}} + \frac{U_\infty f'' A^2}{x^{2n-1}} \frac{\partial \nu_t}{\partial \eta}$$

LET $n = \frac{1}{2}$, $x^{2n-1} = 1$

WHICH GIVES

$$-\frac{U_\infty^2 f'' f}{2} = (\nu_t + \nu)\, U_\infty A^2 f''' + U_\infty f'' A^2 \frac{\partial \nu_t}{\partial \eta}$$

Devide by $U_\infty^2/2$

$$-f''f = (\nu + \nu_t)\frac{2A^2}{U_\infty} f''' + \frac{2A^2}{U_\infty} f'' \frac{\partial \nu_t}{\partial \eta}$$

or

$$-f''f = \left(1 + \frac{\nu_t}{\nu}\right) \frac{2A^2\nu}{U_\infty} f''' + \frac{2A^2\nu}{U_\infty} f'' \frac{\partial(\nu_t/\nu)}{\partial \eta}$$

Let $A = \sqrt{\frac{U_\infty}{\nu}}$, $\eta = y\sqrt{\frac{U_\infty}{\nu x}}$

$$-\frac{f''f}{2} = \left(1 + \frac{\nu_t}{\nu}\right) f''' + f'' \frac{\partial(\nu_t/\nu)}{\partial \eta}$$

APPENDIX C

COMPUTER PROGRAM

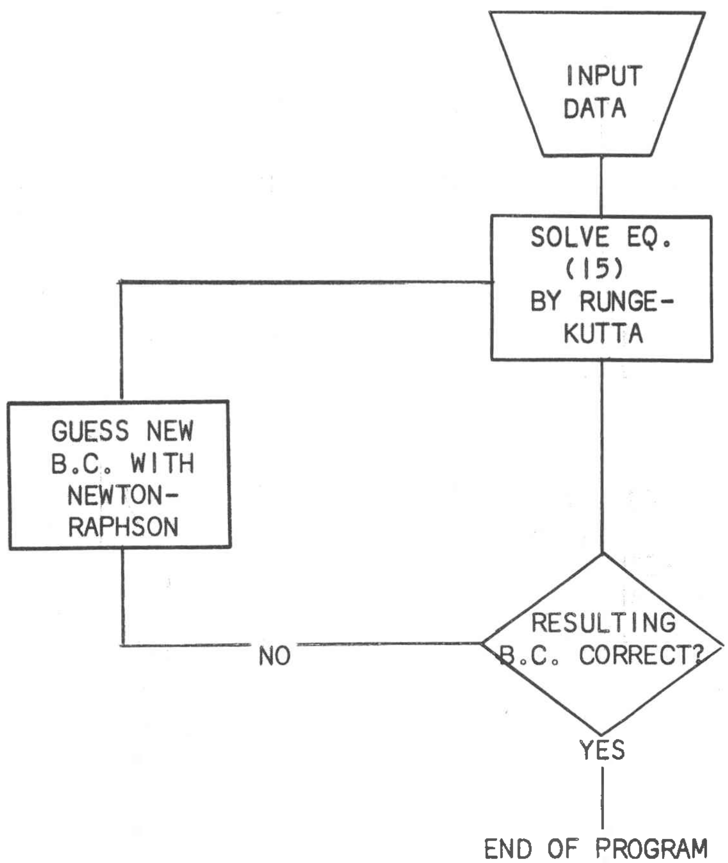

The input to the program includes the $\frac{\xi}{L}$, η variation, the step size, and the definition of the edge of the boundary layer. Equation (15) is solved numerically by a fourth order Runge-Kutta method and the resulting boundary conditions are then checked to see if they are correct. If so, the computation is completed. If not, a new guess for the initial conditions is made by the Newton-Raphson method and the program is repeated until the desired solution is obtained. For a full explanation of the Runge-Kutta method used with all subroutines associated with it see Carnahan [12]. And for a full explanation of the Newton-Raphson method used in the program see Scarborough and Blake [14], and Middlecoff [13]. A listing of the computer program follows.

```
      MAIN DECK
      DIMENSION Y(6),SAVEY(6),PHI(6),F(6),YINT(6),YSAVE(6)
      N=3
      READ(5,100) H,XMAX
  100 FORMAT (2F10.5)
    1 READ (5,80) E1,E2,E3
   80 FORMAT (3F10.5)
      WRITE (6,90) E1,E2,E3
   90 FORMAT (1H1,3F20.5)
      XINT=0.0
      X=XINT
      Y(1)=0.0
      Y(2)=0.0
      Y(3)=2.0
      Y(4)=0.0
      Y(5)=0.0
      Y(6)=0.0
      DO 500 K=1,6
  500 YINT(K)=Y(K)
      CALL RUNGE (H,X,XMAX,IFREQ,Y,E1,E2,E3)
      ERROR=Y(2)-1.000000
      ERROR=ABS(ERROR)
      IF (ERROR.LT.0.00001) GO TO 700
      CALL NR11 (Y,H,YINT,YSAVE,XINT,X)
      CALL RUNGE (H,X,XMAX,IFREQ,Y,E1,E2,E3)
      ERROR=Y(2)-1.000000
      ERROR=ABS(ERROR)
      IF (ERROR.LT.0.00001) GO TO 700
      CALL NR12 (Y,H,YINT,YSAVE,PHINEW,XINT,X)
      CALL RUNGE (H,X,XMAX,IFREQ,Y,E1,E2,E3)
      ERROR=Y(2)-1.000000
      ERROR=ABS(ERROR)
      IF (ERROR.LT.0.00001) GO TO 700
  600 CONTINUE
      CALL NR21 (Y,H1,YINT,YSAVE,PHINEW,PHIOLD,XINT,X)
      CALL RUNGE (H,X,XMAX,IFREQ,Y,E1,E2,E3)
      ERROR=Y(2)-1.000000
      ERROR=ABS(ERROR)
      IF (ERROR.LT.0.00001) GO TO 700
      CALL NR22 (Y,H1,YINT,PHIOLD,XINT,X)
      CALL RUNGE (H,X,XMAX,IFREQ,Y,E1,E2,E3)
      ERROR=Y(2)-1.000000
      ERROR=ABS(ERROR)
      IF (ERROR.LT.0.00001) GO TO 700
      GO TO 600
  700 CONTINUE
      GO TO 1
    2 CONTINUE
      STOP
      END
      SUBROUTINE RUNGE (H,X,XMAX,IFREQ,Y,E1,E2,E3)
      DIMENSION Y(6),SAVEY(6),PHI(6),F(6)
      N=3
      IC=0
```

```
      JC=0
       KC=0
      LC=0
      MC=0
    1 CONTINUE
      CALL FUNC (X,Y,F,E1,E2,E3)
      CALL PASS2 (Y,SAVEY,PHI,F,N,H,X)
      CALL FUNC (X,Y,F,E1,E2,E3)
      CALL PASS3 (Y,SAVEY,PHI,F,N,H)
      CALL FUNC (X,Y,F,E1,E2,E3)
      CALL PASS4 (Y,SAVEY,PHI,F,N,H,X)
      CALL FUNC (X,Y,F,E1,E2,E3)
      CALL PASS5 (Y,SAVEY,PHI,F,N,H)
      CALL RECORD (IC,JC,KC,LC,MC,X,Y(1),Y(2),Y(3))
      CONTINUE
      IF (X.GE.XMAX) GO TO 4
      GO TO 1
    4 CONTINUE
      RETURN
      END
      SUBROUTINE FUNC (X,Y,F,E1,E2,E3)
      DIMENSION Y(6),F(6)
      CALL NU (X,E1,E2,E3,G)
      CALL PARNU (X,E1,E2,E3,P)
      F(1)=Y(2)
      F(2)=Y(3)
      F(3)=-Y(3)*P/G-(Y(1)*Y(3))/((2.0)*G)
      F(4)=Y(4)
      F(5)=Y(5)
      F(6)=Y(6)
      RETURN
      END
      SUBROUTINE PASS2 (Y,SAVEY,PHI,F,N,H,X)
      DIMENSION Y(N),SAVEY(N),PHI(N),F(N)
      DO 1 J=1,N
    1 SAVEY(J)=Y(J)
      DO 2 J=1,N
    2 PHI(J)=F(J)
      DO 3 J=1,N
    3 Y(J)=SAVEY(J)+0.5*H*F(J)
      X=X+0.5*H
      RETURN
      END
      SUBROUTINE PASS3 (Y,SAVEY,PHI,F,N,H)
      DIMENSION Y(N),SAVEY(N),PHI(N),F(N)
      DO 1 J=1,N
    1 PHI(J)=PHI(J)+2.0*F(J)
      DO 2 J=1,N
    2 Y(J)=SAVEY(J)+0.5*H*F(J)
      RETURN
      END
      SUBROUTINE PASS4 (Y,SAVEY,PHI,F,N,H,X)
      DIMENSION Y(N),SAVEY(N),PHI(N),F(N)
      DO 1 J=1,N
```

```
1   PHI(J)=PHI(J)+2.0*F(J)
    DO 2 J=1,N
2   Y(J)=SAVEY(J)+H*F(J)
    X=X+0.5*H
    RETURN
    END
    SUBROUTINE PASS5 (Y,SAVEY,PHI,F,N,H)
    DIMENSION Y(N),SAVEY(N),PHI(N),F(N)
    DO 1 J=1,N
1   PHI(J)=PHI(J)+F(J)
    DO 2 J=1,N
2   Y(J)=SAVEY(J)+(PHI(J))*H/6.0
    RETURN
    END
    SUBROUTINE NU (X,E1,E2,E3,G)
    IF (X.GT.E1) GO TO 1
    G=0.0
    GO TO 2
1   IF (X.GT.E3) GO TO 3
    G=((E3/(E2-E1))-E1)*X+1.0
    GO TO 2
3   G=E3
2   CONTINUE
    RETURN
    END
    SUBROUTINE PARNU (X,E1,E2,E3,P)
    IF (X.LT.E1) GO TO 1
    IF (X.GT.E3) GO TO 1
    P=E3/(E2-E1)
    GO TO 2
1   P=0.0
2   CONTINUE
    RETURN
    END
    SUBROUTINE RECORD (IC,JC,KC, LC,MC,X,A,B,C)
    IC=IC+1
    IF(IC.LT.6) GO TO 1
    IF(IC.LT.51) GO TO 2
    IF(IC.LT.501) GO TO 3
    IF(IC.LT.5001) GO TO 4
    GO TO 5
2   JC=JC+1
    IF(JC.EQ.5) GO TO 6
    GO TO 100
6   JC=0
    GO TO 1
3   KC=KC+1
    IF(KC.EQ.50) GO TO 7
    GO TO 100
7   KC=0
    GO TO 1
4   LC=LC+1
    IF(LC.EQ.500) GO TO 8
    GO TO 100
```

```
    8 LC=0
      GO TO 1
    5 MC=MC+1
      IF(MC.EQ.5000) GO TO 9
      GO TO 100
    9 MC=0
      GO TO 1
    1 WRITE (6,402) X,A,B,C
  402 FORMAT (1H0,4F10.5)
  100 CONTINUE
      RETURN
      END
      SUBROUTINE NR11(Y,H,YINT,YSAVE,XINT,X)
      DIMENSION Y(6),YINT(6),YSAVE(6)
      DO 1 K=1,6
    1 YSAVE(K)=Y(K)
      DO 2 K=1,6
    2 Y(K)=YINT(K)
      Y(3)=YINT(3)+H
      X=XINT
      RETURN
      END
      SUBROUTINE NR12 (Y,H,YINT,YSAVE,PHINEW,XINT,X)
      DIMENSION Y(6),YINT(6),YSAVE(6)
      PHIOLD=YSAVE(2)-1.000000
      PHINEW=Y(2)-1.000000
      DPHI=(PHINEW-PHIOLD)/H
      DY=-PHIOLD/DPHI
      YINT(3)=YINT(3)+DY
      DO 1 K=1,6
    1 Y(K)=YINT(K)
      X=XINT
      RETURN
      END
      SUBROUTINE NR21 (Y,H1,YINT,YSAVE,PHINEW,PHIOLD,XINT,X)
      DIMENSION Y(6),YINT(6),YSAVE(6)
      DO 1 K=1,6
    1 YSAVE(K)=Y(K)
      PHIOLD=YSAVE(2)-1.000000
      H1=-PHIOLD/PHINEW
      DO 2 K=1,6
    2 Y(K)=YINT(K)
      Y(3)=YINT(3)+H1
      X=XINT
      RETURN
      END
      SUBROUTINE NR22 (Y,H1,YINT,PHIOLD,XINT,X)
      DIMENSION Y(6),YINT(6)
      PHINEW=Y(2)-1.000000
      DPHI=(PHINEW-PHIOLD)/H1
      DY=-PHIOLD/DPHI
      YINT(3)=YINT(3)+DY
      DO 1 K=1,6
    1 Y(K)=YINT(K)
      X=XINT
      RETURN
      END
```

LIST OF REFERENCES

1. Prandtl, L. Recent Results of Turbulence Research. NACA TM 720. 1933.

2. von Karman, Th. Nachr. Ges. Wiss. Gottingen. 58-76. 1930.

3. Nikuradse, J. VDI-Forschungsh. no. 356. 1932.

4. Millikan, C.B. A Critical Discussion of the Turbulent Flows in Channels and Circular Tubes. Proc. Fifth Intern. Congress Appl. Mech. Cambridge, Mass. 386-392. 1938.

5. Kestin, J., and Richardson, P.D. Heat Transfer Across Turbulent, Incompressible Boundary Layers. Int. J. Heat Mass Transfer. 6:147-189. 1963.

6. Martinelli, R.C. Heat Transfer to Molten Metals. Trans. ASME. 69:947-959. 1947.

7. Deissler, R.G. Analytical and Experimental Investigation of Adiabatic Turbulent Flow in Smooth Tubes. NACA TN 2138. July, 1950.

8. Van Driest, E.R. Heat Transfer Fluid Mech. Inst. Paper XII. 1955.

9. Spalding, D.B. Heat Transfer to a Turbulent Stream from a Surface with a Step-wise Discontinuity in Wall Temperature. ASME Conference. Intern. Dev. in Heat Trans. Boulder, Colo. Part II:439-466. 1961.

10. Schlichting, H. Boundary Layer Theory. McGraw-Hill, New York. 1960.

11. Hinze, J.O. Turbulence. McGraw-Hill, New York. 1959.

12. Carnahan, B., Luther, H.A., and Wilkes, J.O. Applied Numerical Methods. John Wiley and Sons, New York. 1964.

13. Blake, L.H., and Middlecoff, J.F. Newton-Raphson Solution to Boundary Value Problems with Variable Incremental Approximation. Lockheed Palo Alto Research Laboratory, Palo Alto, Calif. 1967.

14. Scarborough, J.B. Numerical Mathematical Analysis. Oxford University Press. 1962.

15. Schultz-Grunow, F. New Frictional Resistance Law for Smooth Plates. NACA TM 986. 1941.

16. Schubauer, G.B., and Tchen, C.M. Turbulent Flow. Princeton University Press, Princeton, New Jersey. 1961.

17. Clauser, F.H. The Turbulent Boundary Layer. Advances in Applied Mechanics. 4:1-51. 1956.

A SIMILARITY MODEL FOR FLOW IN A TURBULENT BOUNDARY LAYER

An Abstract of a Thesis

Presented to

The Department of Mechanical Engineering Science

Brigham Young University

In Partial Fulfillment

of the Requirements for the Degree

Master of Science

by

E. Clark Lemmon

May 1968

ABSTRACT

The purpose of this thesis was to reduce the governing equation for flow over a flat plate which is a partial differential equation to an ordinary differential equation by a similarity solution, and then numerically solve the obtained transformed governing equation. The solution of this equation was found to be dependent on the modeling of the variation of the eddy diffusivity across the boundary layer. The results obtained by numerically solving the transformed governing equation were compared with experimental data. The predicted profile compared very well with the experimental profile near the wall and in the turbulent core. However, the agreement in the buffer region was poor. The results obtained implied that a better fit could be obtained if a more complex model of eddy diffusivity as a function of position were used.

APPROVED: